COMPRESSION-AIDED STABILITY OF ORTHOPAEDIC DEVICES

A Thesis
Presented to
The Academic Faculty

By

Mary Katlyn Pitz

In Partial Fulfillment
Of the Requirements for the Degree
Master of Science in BioEngineering

Georgia Institute of Technology

May 2011

COMPRESSION-AIDED STABILITY OF ORTHOPAEDIC DEVICES

Approved by:

Dr. Kenneth Gall, Advisor
School of Material Science and Engineering
Georgia Institute of Technology

Dr. David McDowell
The George W. Woodruff School of Mechanical Engineering
Georgia Institute of Technology

Dr. J. Kurt Jacobus
MedShape Solutions

Date Approved: December 20, 2010

ACKNOWLEDGEMENTS

I would first and foremost like to thank MedShape Solutions for providing the environment, the technology, and the funding that was essential to my research. Thank you to Dr. Ken Gall for providing me the unique opportunity to intern at MedShape, and for the subsequent support and guidance that resulted in this thesis. I'd also like to acknowledge my committee members, Dr. David McDowell and Dr. Kurt Jacobus for volunteering their time and expertise. I truly appreciate your willingness to serve on my committee and your response to and opinions on the work presented.

Thanks to all MedShapers, each of whom has in some way provided support to me over the past few years. I needed all of the advice, the cookies, the laughs, and practical jokes to survive. I appreciate the wisdom and figures provided to me by Dr. Chris Yakacki. Thank you especially to Katy Shaffer who knew just as much about the trials and tribulations I faced as I did, and who reminded me consistently that there was a light at the end of the tunnel.

Thank you to the Gall Lab for giving me a desk and treating me like a labmate even though my time was often spent at MedShape--particularly to Kathryn Smith, David Safranski, and Walter Voit for always being willing to lend a helping hand, a lab key, or a furnace.

Finally, I'd like to thank all of my family and friends for supporting me for the duration of this process. I love you all and couldn't have done it without you.

TABLE OF CONTENTS

LIST OF TABLES

LIST OF FIGURES

LIST OF ABBREVIATIONS

IM	intramedullary
m	meter
mm	millimeter
N	Newton
Ni	Nickel
Nitinol	Nickel-Titanium
pcf	pounds per cubic foot
Ti	Titanium
TTC	tibiotalocalcaneal

SUMMARY

Repair and remodeling of bone during healing and fusion require a combination of bone resorption and formation to successfully restore the bone to its previous strength. The healing process is highly responsive to the mechanical conditions of the construct, where excessive loading can cause high strains that delay healing, but moderate loading can be beneficial. Maintaining compression at the site of fracture can benefit healing by maintaining bone congruency and increasing the stability of the bone-implant construct to prevent excessive shifting. For these reasons, compressive mechanisms are employed in many orthopaedic devices, including both intramedullary (IM) nails and external fixators for ankle arthrodesis applications. Tibiotalocalcaneal (TTC) arthrodesis is a salvage procedure that fuses both the ankle and the subtalar joints. It has become the standard of care in ankle degeneration, which can be brought on by posttraumatic arthritis, failed total ankle arthroplasty, or diabetic conditions such as Charcot arthropathy. While current devices are effective in many cases, TTC arthrodesis procedures still incur failure rates as high as 22%, where failure of the bones to successfully fuse can result in amputation. Because bone healing relies upon bone resorption, the initial compression applied to the implanted constructs can be quickly lost, which may sacrifice the stability of the structure and delay or inhibit further healing.

By employing a mechanism that can sustain compression during the bone healing process, it may be possible to increase the stability of the construct even during bone resorption, minimizing the failures that still occur. The focus of this study was to determine the effects of compression on the mechanical stability of the implant-bone construct found in TTC arthrodesis. A comparison was made between the torsional stability of two currently marketed intramedullary devices, as well as a prototype IM device comprised of a nickel titanium core, designed to hold constant compression for up to 9mm of resorption. Additionally, the stability of

each construct over time was evaluated by correlating bone resorption to a loss in compressive force.

CHAPTER 1

INTRODUCTION

1.1 Ankle Arthrodesis

Tibiotalacalcaneal (TTC) arthrodesis is a salvage procedure that fuses both the ankle (the joint space connecting the tibia and talus) and the subtalar (between the talus and calcaneus) joints. Figure 1 shows the bony anatomy of the ankle. First described in 1882 by Eduard Albert, TTC arthrodesis has become a standard treatment for care in ankle degeneration [1]. Successful ankle fusion aims to relieve patients from painful ankle conditions that range from degenerative osteoarthritis, failed total ankle arthroplasty, posttraumatic injury, and diabetic conditions such as Charcot arthropathy [2-6]. Though the intent of the outcome is dependent upon the condition necessitating the procedure, TTC arthrodesis universally aims to achieve hindfoot alignment via union at the joints while avoiding potential complications [7].

Because ankle arthrodesis is indicated by a number of conditions, the population of patients who undergo the procedure varies greatly. Arthritis is one of the common indications for the procedure. Unlike the hip or knee, which can be affected by primary osteoarthritis, the ankle joint is most commonly vulnerable to secondary, or posttraumatic, arthritis. Seventy percent of ankle osteoarthritis is the result of an initial trauma [1, 6]. This serves to vary the patient profile as younger patients, who are typically not hindered by primary arthritis, can be subject to this procedure as a result of posttraumatic arthritis. Diabetic conditions, such as Charcot neuropathy, however, indicate a slightly older population. As such, published data from clinical ankle arthrodesis studies have an average age ranging from 40-60 years old, while the individual patient age ranges from 19 to 88 years [2-5, 8-10]. Similarly, there is no definite inclination toward a male or female population [2-3, 10] in ankle arthrodesis procedures.

As a salvage procedure, ankle arthrodesis is typically only attempted after other non-surgical options, such as ambulatory bracing, have been exhausted [4, 8]. Once surgical

intervention is deemed necessary, ankle arthrodesis is recognized as the most durable and widely accepted treatment for osteoarthritis of the ankle [11]. Other options include ankle joint replacement arthroplasty, ankle distraction arthroplasty or amputation [1]. Because ankle fusion is a last-ditch attempt at providing patients functional independence in light of their conditions, repeated failure of arthrodesis can lead to amputation.

The array of conditions that lead to TTC arthrodesis as well as slight variations in ankle arthrodesis procedures (where different joints can be fused in the hindfoot) make it difficult to compile statistics as to the prevalence of this procedure. In the absence of these, it can be difficult to find motivation in improving current technology. In the case of ankle arthrodesis however, the motivation to ensure the highest possible success rate in ankle fusion is the desire to avoid the devastating results from failure of the procedure. Each successful ankle fusion represents a patient who is spared amputation and the devastating effects it would cause to his daily life.

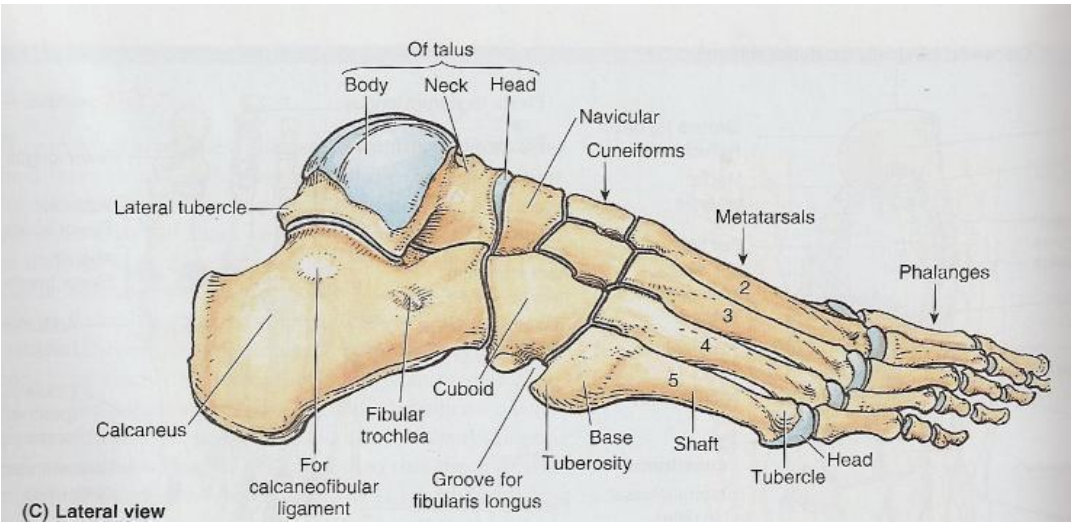

Figure 1 (a). Anatomy of the bones of the foot [12].

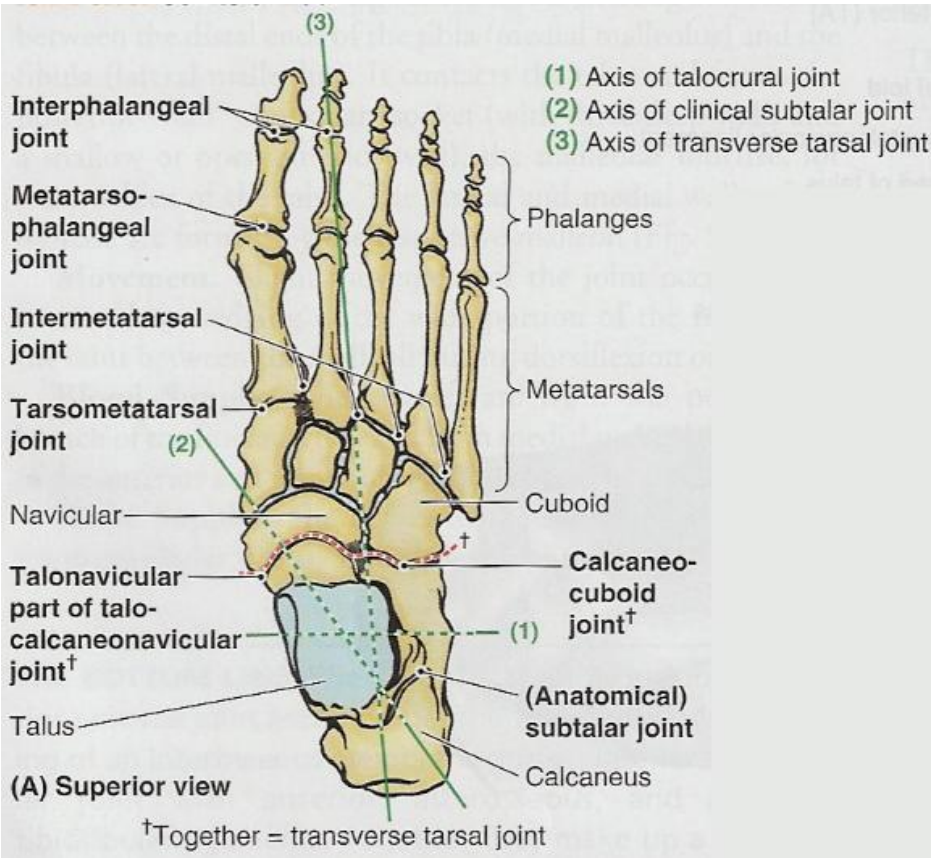

Figure 1 (b). Anatomy of the joints of the foot [12].

1.2 Bone Healing

The process by which bones fuse is thought to be similar to the process of healing in long bones [13]. Long bones can heal via primary or secondary healing. In primary healing, the outer layer of bone--the cortex--from one side of the fracture or fusion site unites directly with the cortex of other side. This only occurs in situations of extremely rigid fixation where the fracture is stable and interfragmentary strain is low. Secondary healing occurs in situations of less rigid fixation and involves the classic stages of healing characterized by callus formation and ultimately, bony union. Those classic healing stages can be broken down into three parts, including early inflammation, repair, and remodeling [14]. During inflammation, granulation tissue is formed and the groundwork is laid to promote later vascularization of the fusion space. In the repair stage, vascularization further progresses while a collagen matrix is laid down via

osteoid that is secreted and mineralized. This results in a soft callus at the site of repair for 4-6 weeks. If the soft callus has been sufficiently protected from motion for the duration of this period, it will ossify, thus bridging the gap between the bony ends with woven bone. Finally, remodeling takes place in which the bone returns to its previous strength and adapts its shape to support the mechanical loads placed upon it.

Bone remodeling relies on the different types of bone cells—osteocytes, osteoclasts, and osteoblasts--to work together as a basic multicellular unit (BMU) to resorb old and lay new bone. Osteoclasts are responsible for the resorption of old bone. Derived from the same lineage as macrophages, osteoclasts first form a tight seal with the calcified matrix and then secret hydrolytic enzymes to break down the calcified matrix of bone. Osteoblasts are responsible for new bone generation; they lay the extracellular matrix and regulate its mineralization. Osteocytes are mature osteoblasts that have become embedded the bone mineral matrix. Osteocytes are the most abundant cell in bone, and as such are thought to be sensitive to mechanical stimuli and able to communicate with and recruit other bone cells through the internal architecture of the bone [15].

Throughout the bone healing, fusion, and remodeling processes, the bone is responsive to hormonal, chemical, and mechanical signals. First discovered by and widely recognized as Wolff's law, the concept that functional changes in loading result in adaptive architectural and structural changes is particularly effective here. Mechanical stimulus is recognized to promote osteogenesis on both a cellular and systemic level. In vitro studies have demonstrated that application of strain, fluid shear stresses, or hydrodynamic loading are effective in directing cell differentiation or stimulating already differentiated cells to secrete specific matrix components [16]. Systemically, clinical studies that have monitored bone healing as a function of different mechanical stimuli demonstrate increased callus formation in the mechanically stimulated groups [17]. These clinical studies also made evident that high strains during early phases of healing can promote callus formation while the same high strains can be inhibitive in later

stages of remodeling. Additionally, these studies have demonstrated that fracture healing is hampered by increased fracture gaps, where 2mm can circumvent healing [16-18].

1.3 Compression

Applying compressive force at the site of bone fracture or fusion to enhance bone healing logically follows many of the bone healing principles. The application of compression increases the stability of the fracture, encouraging bone healing to take place. Allowing for a joint connection with compression maintains joint congruency and the alignment that the surgeon has created during reduction [16]. Because fracture gaps of 2mm or greater are known to inhibit callus formation and subsequent fracture healing, compression helps to minimize rotational and axial motion, thus maintaining optimal positioning. In addition to the mechanical stability compression can offer to the construct, the application of compression can be instrumental in supplying some level of mechanical stimulation to the fracture site, encouraging healing.

The potential benefits of employing compression in fracture fixation and particularly ankle arthrodesis devices have been recognized and put into effect. Compression arthrodesis was first described by Charnley in 1951 [10]. Charnley described compression arthrodesis as achieving “direct union…between the living bones forming the joint surfaces without the intervention of an inert graft.” He went on to state that, “one of the effects of compression is to eliminate all shearing strains as well as preventing a gap between the cut bone surfaces [19].” Though Charnley addressed these concerns in 1951, current knowledge regarding bone healing and fusion remains consistent with his statements. As such, surgical techniques and devices have evolved from Charnley’s first described method of external fixation that added compression via two parallel pins inserted laterally through the tibia, but continue to employ the compression that he advised [19]. These advanced techniques and devices have included pinning, plating, external fixation, and internal fixation via crossed cancellous screws or intramedullary nailing. Among these, hip pinning is found to lose alignment and result in

malunion while plating is undesirable because it requires extensive soft tissue dissection [7]. External fixation and internal fixation (via cancellous screws or intramedullary nailing) remain the most common methods to achieve arthrodesis today. While the techniques differ, they universally aim to use compression at the fusion site to stimulate bony union and provide rigid fixation. Both clinical and biomechanical studies have been undertaken to determine the effectiveness of different devices and whether one can be considered the superior means of fixation.

1.4 Clinical Devices

Multiple clinical and biomechanical studies have been focused on determining the best method of fixation. Fixation methods are assessed based on critical factors in fixation, including the length of the non-weight bearing period after surgery, the time it takes to achieve bony union at the fusion site, the rate of nonunion, and the infection rate. In general, the post-surgical non-weight bearing period can last anywhere from 6-12 weeks, successful fusion typically occurs between 12 and 20 weeks, and nonunion rates occur in about 15% of cases studied.

External fixation has evolved since Charnley first described it in his 1951 paper, but the basic principles remain fundamentally unchanged. Charnley passed pins through distal and proximal portions of the fusion site and compressed them using externally located clamps. The device he employed had good results, but poor rotational stability [10]. Improvements have been made through the use of triangular frames that offer multiplanar compression. These devices offer the benefits of dynamic axial fixation that can be adjusted throughout the healing process [11]. Additionally, they have excellent bending, shear, and torsional stability which allow for early weight-bearing during the patient's postoperative period. The average time to fusion, however, has been found to be 25-28 weeks, which is longer than intramedullary methods [10, 20]. Additional pitfalls of the external fixator are related to the fact that the compressive mechanism is achieved outside of the body. This requires a bulky device to be worn for long

periods of time, which results in poor patient compliance [7, 11, 21]. The fact that the compression pins pass from the external environment through the leg also carries high risk of pin-tract infection, which is a problem in approximately 13% of cases [20]. Because of these shortcomings, external fixation is still a viable option for ankle arthrodesis procedures, but typically reserved for patients with extensive soft tissue injury or infection where internal devices would be inappropriate [21]. When used, current external fixators can have nonunion rates as high as 41% [20].

Internal fixation methods commonly used today include cancellous screws that cross through the joints to be fused and locked intramedullary nails. Configurations of 2 to 3 crossed cancellous screws are used in some arthrodesis procedures. These configurations have been demonstrated to have slightly inferior contact area and bending and torsional stiffness than intramedullary nail configurations [7, 21]. Cancellous screws can have poor stability because of bone defects at the arthrodesis site and are often avoided in situations of poor bone quality because of inadequate stabilization [3].

Intramedullary (IM) nailing was first described by J. Crawford Adams in 1948 as a secondary procedure after a failed attempt at fusion via fibular grafting [22]. At the time, the nail was used to supply rigid immobilization to the construct. Intramedullary nails continue to be used because they can have shorter time to bone union (14 weeks), and because of the stability they can provide. They have evolved since Adams first used them to offer more dynamic healing options. First generation IM nails are static devices that allow for compression by having the surgeon hammer on a strike plate of the installation hardware and subsequently lock the nail in the compressed position. Second generation nails offer a means of applying compression similar to that of external fixators, where pins are passed through the proximal tibia and used to compress the joints together. Importantly, the compression pins are removed in these devices after the second set of screws lock the nail in the compressed position. These nails also offer a slotted proximal locking hole which allows for dynamization of the construct.

Opting for the dynamic configuration, in which the static locking screw is removed in either the original or a subsequent procedure, allows for earlier weight-bearing and eliminates the stress shielding effects that can result from too-rigid devices. A third generation of IM nails have internal mechanisms for compression that offer a degree of dynamic movement equal to the length of the slot the locking screw is engaged in [23].

Clinical and laboratory results have led to the increased dependency on intramedullary nailing for ankle arthrodesis procedures. Further propelling this change is the ability to add dynamic locking to IM constructs, which has been shown to increase load sharing between the hardware and bone, thus decreasing the time to weight bearing. A study of dynamically locked screws found that approximately 2.3mm of movement occurred due to impaction, indicating that dynamic healing was taking place over the course of fusion. Additionally, they found that earlier weight bearing was possible (6 weeks) and time to fusion was generally shorter than other methods at 3.7 months [3].

There is a good understanding of the components necessary to enable solid and rapid union—initial stability, compression, and load sharing to enable early weight bearing. Mueckley recognized that compression mechanisms maintain an average of only 60% of the compression that is initially applied. He was able to increase the average maintained compression in a study where he employed a device with an internal compression mechanism. While this increased compression would benefit the stability of the construct initially, the in-vivo response to resorb bone before forming a new bony callous would result in decreased compression—and thus decreased stability—over time [21]. The addition of *dynamic compression* would allow not only impaction during bone resorption, but would maintain the compression that increases construct stability during bone resorption.

Despite the incremental improvements made in the field with compression and dynamic locking, ankle arthrodesis still experiences failures as high as 22% [9]. These failures can lead to successive attempts at arthrodesis, which are more prone to failure because the bone has

been previously compromised, or ultimately even amputation. The ability to maintain compression throughout the bone resorption that occurs in the bone fusion process would be beneficial for both the longevity of the device and the stability of fixation. After compression is inevitably lost in normal devices during bone healing, the stability of the fusion site is dependent solely upon the hardware's purchase in the bone and its ability to resist micro-motion. In addition to a loss of stability, this places increased force on the hardware itself, which can result in hardware failure. By maintaining compression across the site in the face of bone resorption, the bone is forced to bear some of the load, which stimulates bone healing while simultaneously protecting the hardware.

1.5 NiTiNOL

Nitinol is a nickel titanium alloy with excellent corrosion resistance, wear characteristics, and biocompatibility, making it a popular material for use in medical applications. Nitinol has the added benefit of both shape memory and pseudoelastic properties. The shape memory effect refers to the ability of the material to recover an original shape after deformation at low temperatures. Pseudoelasticity refers to the ability of the material to recover strain produced by a stress-induced phase transformation upon immediate unloading without a temperature increase [24]. When properly tailored, NiTi can exhibit these pseudoelastic properties which are characterized by stress-strain curve similar to the one demonstrated in Figure 2. During loading, the material first goes through elastic deformation, then begins martensitic transformation at point B, which it completes at point C. After point C, the sample will continue to deform elastically until it reaches its yield point. If the sample is unloaded before it yields, it will recover, reversing through the same phases, to nearly zero strain.

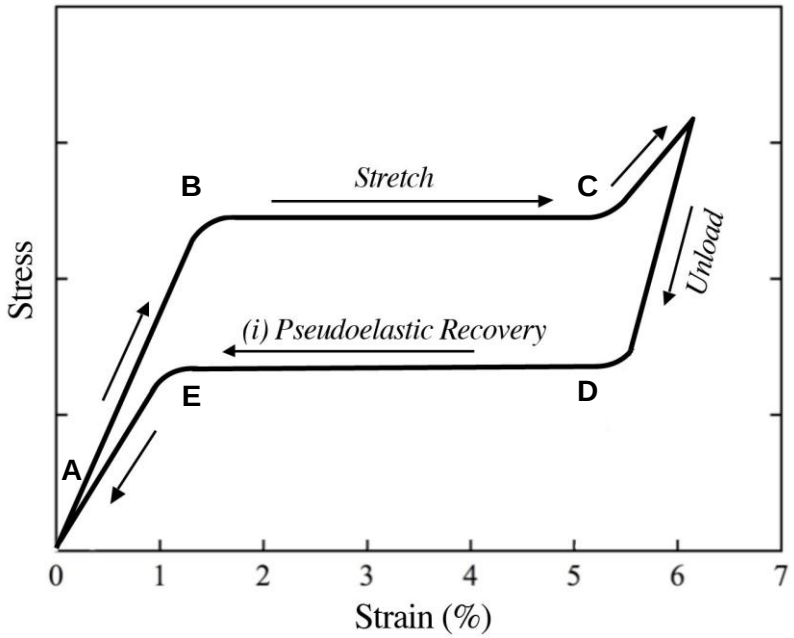

Figure 2. Typical NiTi load/unload curve in the pseudo-elastic regime.

The pseudoelastic capabilities of NiTi make it an attractive option to work into orthopaedic devices as a compressive mechanism, much like third generation intramedullary nails for ankle arthrodesis employ internal screws. The use of NiTi would provide the added benefit of *sustained* compression over the course of the dynamic bone healing process. If the dynamic element is locked at 6% strain along the lower plateau (from D to E), it will supply constant compression at the fusion site in the face of bone resorption until the strain has been fully recovered. The pseudoelasticity of NiTi makes it possible to maintain the *dynamic compression* that could service ankle arthrodesis devices by maintaining the structural rigidity of the complex during healing.

Building on the principles that a dynamic healing environment will be serviced by the ability of a device to offer sustained compression, a prototype device for ankle arthrodesis was created. It features a titanium nail embedded with a thin NiTi core that is stretched and locked at 6% strain during implantation. Current devices offer surgeons the ability to tailor the amount of compression and decide whether axial movement will be accommodated for by locking the

device dynamically. This prototype—Dynanail— allows the surgeon to tailor the amount of initial compression and the level of resorption that will be accommodated for. If the surgeon chooses to allow for resorption, the NiTi core element will be stretched and released so that the load on the lower plateau is maintained. The amount of resorption that can be accommodated for is adjustable by locking the element at various levels of strain along that lower plateau, but this does not affect the compressive force applied by the element. The level of compression and resorption are highly tunable as a combination of manual initial compression and compression via the NiTi core can be chosen. There are three primary insertion scenarios, each of which provides a range of compression:

1. Apply load from the NiTi element with additional manual compression.
2. Apply load from the NiTi element without any additional manual compression.
3. Apply manual compression only (the nail will act as a second generation IM nail).

1.6 Project Aims

The incorporation of compression into all market-leading ankle arthrodesis devices indicates that it is essential to a successful fusion. A further look into the bone healing process suggests that this is the case both because of the mechanical stability compression provides as well as the mechanical stimulus it can generate by maintaining contact between the bone ends. While a study evaluating the effect of compression as mechanical stimulus and thus a promoter of bone healing would be extensive and reliant upon animal models, a study of the effects of compression on the mechanical stability of the construct can be assessed by laboratory model. This study aimed to:

1. Develop a model to evaluate the mechanical stability of an ankle arthrodesis construct.
2. Determine the effects of compression on the mechanical stability of the implant-bone construct in three IM nail devices.
3. Evaluate stability of the construct over time by correlating bone resorption to loss in compression.

CHAPTER 2

EXPERIMENTAL METHODS

2.1 Synthetic Polyurethane Model

The impact of compression on torsional stability in tibiotalocalcaneal arthrodesis was assessed in three intramedullary ankle fusion devices. Two of the three devices, Versanail (DePuy, Warsaw, IN) and Pantanail (Integra, Plainsboro, NJ), are commercially available products for tibiotalocalcaneal arthrodesis procedures. The third device, Dynanail, is a prototype device that employs an internal nickel titanium compression mechanism.

Each device was tested in two scenarios—a simulation of bone resorption and a model of torsion where torque was applied via load at the end of a lever arm. For each, the respective nails were implanted in synthetic polyurethane constructs and secured by a total of four screws--two screws engaged in the “calcaneus” and two screws located proximally in the “tibia.” Synthetic polyurethane from Sawbones (Vashon, WA) has been used previously for biomechanical studies to simulate the properties of real bone while minimizing the variability that would inevitably be present in cadaver bone [21, 23]. In this study, 20pcf solid polyurethane foam was cut to 1.5” x 1.5” squares of varying lengths. A 1” length piece was used to represent the talus, a 5” length was used to represent the calcaneus and a 7” length was used to represent the tibia. Holes were drilled in the sawbone according to the recommendation made in the surgical techniques. The devices were implanted in the sawbone using the recommended instrumentation sets as suggested in the surgical protocol. The parameters used for each device implantation are noted in Table 1.

Table 1. Parameters of implantation for each device used.

Parameter	Versanail	Pantanail	Dynanail
Nail Length	200 mm	180 mm	220 mm
Nail Diameter (Proximal/Distal)	10mm / 12mm	11 mm / 11mm	10mm/ 12mm
Thru Hole Diameter (Proximal/Distal)	10.5/12.5mm	11.5mm	10.5/12.5 mm
Primary screw orientation	Medial-lateral	Posterior-anterior	Medial-lateral
Screw diameter (Calcaneal/Tibial)	5.5mm/4.5mm	5 mm/5mm	4.6 mm/4.6 mm

2.2 Resorption Measurements

Bone resorption was simulated in the manner previously described by Yakacki et al by inserting a set of parallel plates separated by adjustable screws in the sawbone-nail construct [23]. A donut load cell (Transducer Techniques) was used to measure the compressive load throughout the resorption process. Both the resorption plate and load cell were placed around the nail and between the two sets of screws maintaining the compression within the construct. This configuration is shown in Figure 3. The compressive load was monitored as the screws were turned to reduce the distance between the plates. The distance between the plates was uniformly decreased as a function of the screw pitch and confirmed with caliper measurements (Mitutoyo Digital Calipers).

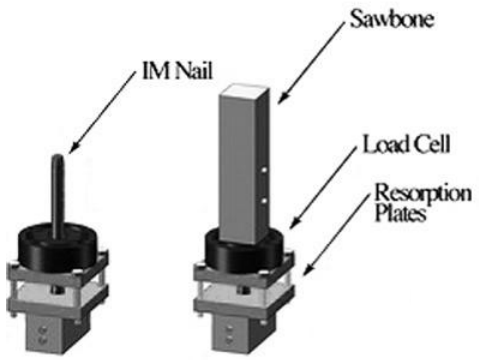

Figure 3. Schematic of bone resorption model.

The loading conditions for Versanail and Pantanail were straightforward, as all of the allowable compression was applied manually during implantation. To assess resorption over the widest range possible, both Versanail and Pantanail were loaded to the maximum compressive force achievable before resorption measurements began. Resorption was measured for four initial loading conditions of the Dynanail device based on the ability to apply compression with a combination of manual force and the NiTi element. The loading scenarios tested are outlined in Table 2. A minimum of two samples were tested for each construct, and a third was tested in situations without good agreement between the first two samples. The resulting curves from this process were able to relate the compressive load to a particular level of resorption for each of the three nails.

Table 2. Loading scenarios for resorption testing in each device**.**

Versanail	Pantanail	Dynanail
Maximum Compression	Maximum Compression	NiTi: Active Manual Compression: Maximum
		NiTi: Active Manual Compression: 600N
		NiTi: Active Manual Compression: None
		NiTi: Not Active Manual Compression: Maximum

2.3 Torsional Stability

Torsional stability was assessed by measuring compressive force versus extension with force application at the end of a lever arm that resulted in a moment about the nail. In this construct, bone block was used to represent the tibia, talus, and calcaneus. Additionally, the donut load cell was included to measure the compressive force within the construct prior to, during, and after testing. Bending of the construct was minimized by fixing the bone block to the Instron base with the exception of one joint, where rotation of sawbone against sawbone took place under the applied load. Load was applied at the end of a 90mm lever arm via the Instron Universal Tensile Testing machine. The test setup is demonstrated in Figure 4, where the blue arrow indicates the application of load. The black arrows show where the sawbone blocks were fixed to the base.

Each sample was loaded in compression at a rate of 0.5mm/second. Extension was plotted versus the applied load for extension up to 25 mm and for the subsequent unloading, at the same rate, to 5 Newtons.

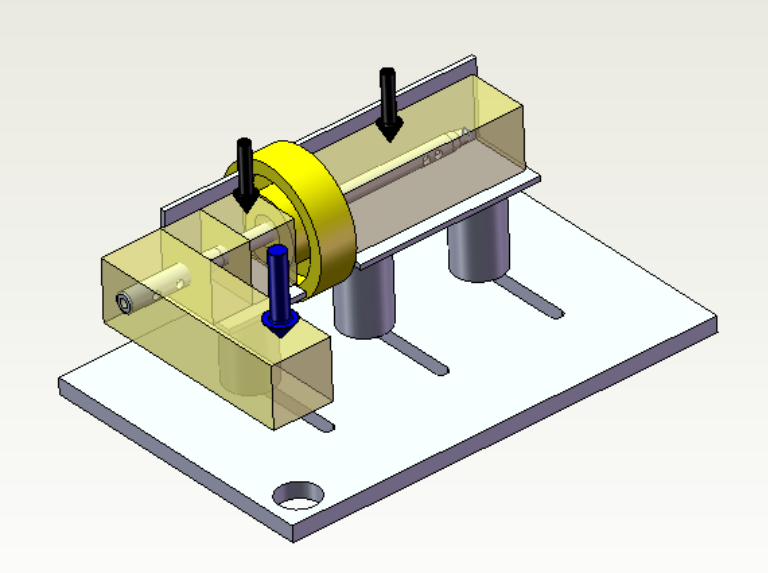

Figure 4. Schematic of torsional stability model.

To evaluate the effect of compression on torsional stability, a variety of loading scenarios were tested for each nail. Each nail was tested in maximum compression, under no compression, and in two intermediate loading scenarios which were dictated by the device and its limits. The loading scenarios for each are outlined in Table 3. Each configuration was tested a minimum of three times, with a unique device implantation each time.

Table 3. Loading scenarios for torsional stability testing in each device.

Loading Scenario	Versanail	Pantanail	Dynanail
Maximum Compression	Maximum Compression *Average: 316 N*	Maximum Compression *Average: 1048 N*	NiTi: Active Manual Comp: Max *Average: 1294 N*
High Compression	Target: 200 N *Average: 271 N*	Target: 750 N *Average: 735 N*	NiTi: Active Manual Comp: 600 N *Average: 539 N*
Low Compression	Target: 100 N *Average: 109 N*	Target: 350 N *Average: 363 N*	NiTi: Active Manual Comp: None *Average: 475 N*
No Compression	No Compression	No Compression	No Compression

CHAPTER 3

EXPERIMENTAL RESULTS

3.1 Resorption Curves

Figure 5 shows a representative resorption curve for the each three IM devices in their configurations of maximum compression, which are the most likely to be used in surgery. The initial portion of the curve for all three devices is characterized by dramatic losses in load over small resorptive distances. For Pantanail and Versanail, which employ only manual compression applied with the instrumentation at the time of loading, this trend continues until all compression is lost. In these devices, that loss of compression occurs in only 0.5 to 1.5 mm of resorption. The Dynanail device, however, reaches a plateau at the load level equal to that of the plateau in the NiTi unloading curve. Once this load is reached, it is maintained until the NiTi element is fully unloaded. This orientation of the Dynanail device maintains compression over 8mm of resorption. These curves demonstrate that configurations with higher initial loads are able to maintain compression for slightly higher levels of resorption, but the addition of the pseudoelastic element dramatically increases the ability of the construct to maintain compression.

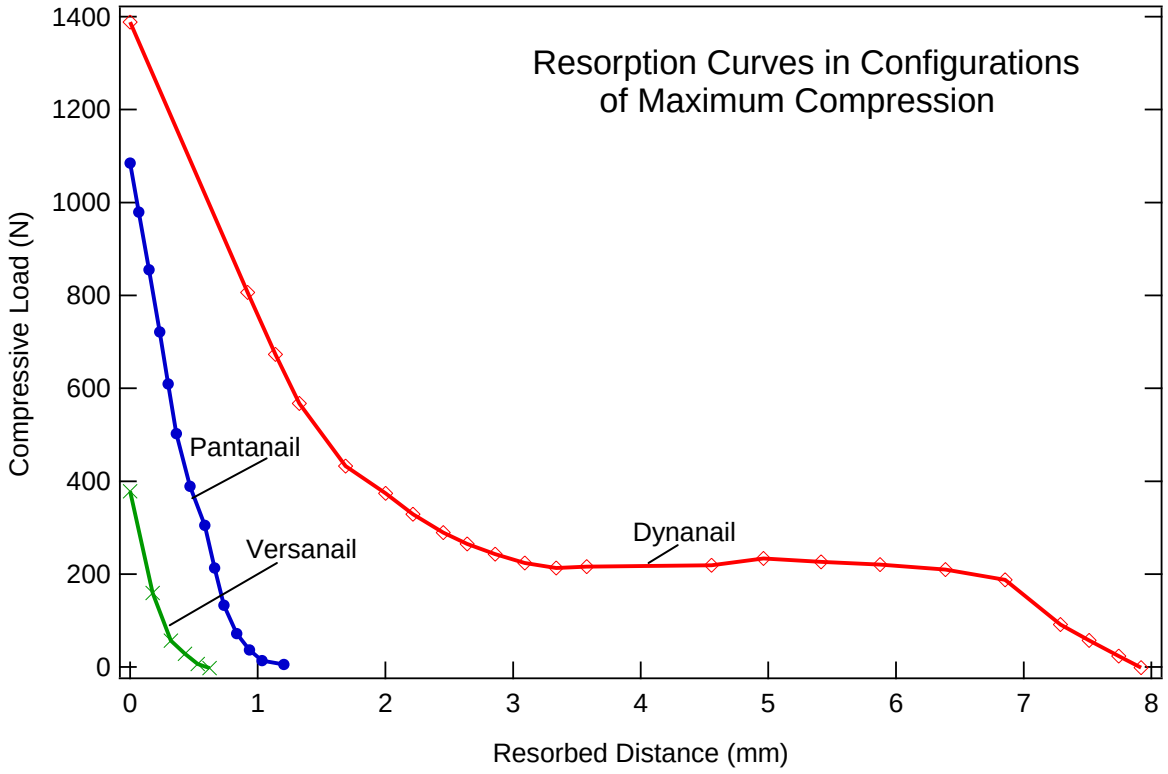

Figure 5. Resorption curves for all devices in configurations of maximum compression.

Figure 6 shows the resorption curves for the various loading configurations possible in the Dynanail device. Depending on the method of implantation, the initial compressive values for Dynanail range from 334N when compression is added manually without activating the NiTi core at all to 1449N when the NiTi core is activated in conjunction with manual compression. The initial loss of load in the maximum compression scenario follows the same trajectory as the sample loaded without NiTi activation. This indicates that until the compressive force is reduced to the level sustained by the NiTi itself, compression is lost in the same manner as other non-dynamic nails.

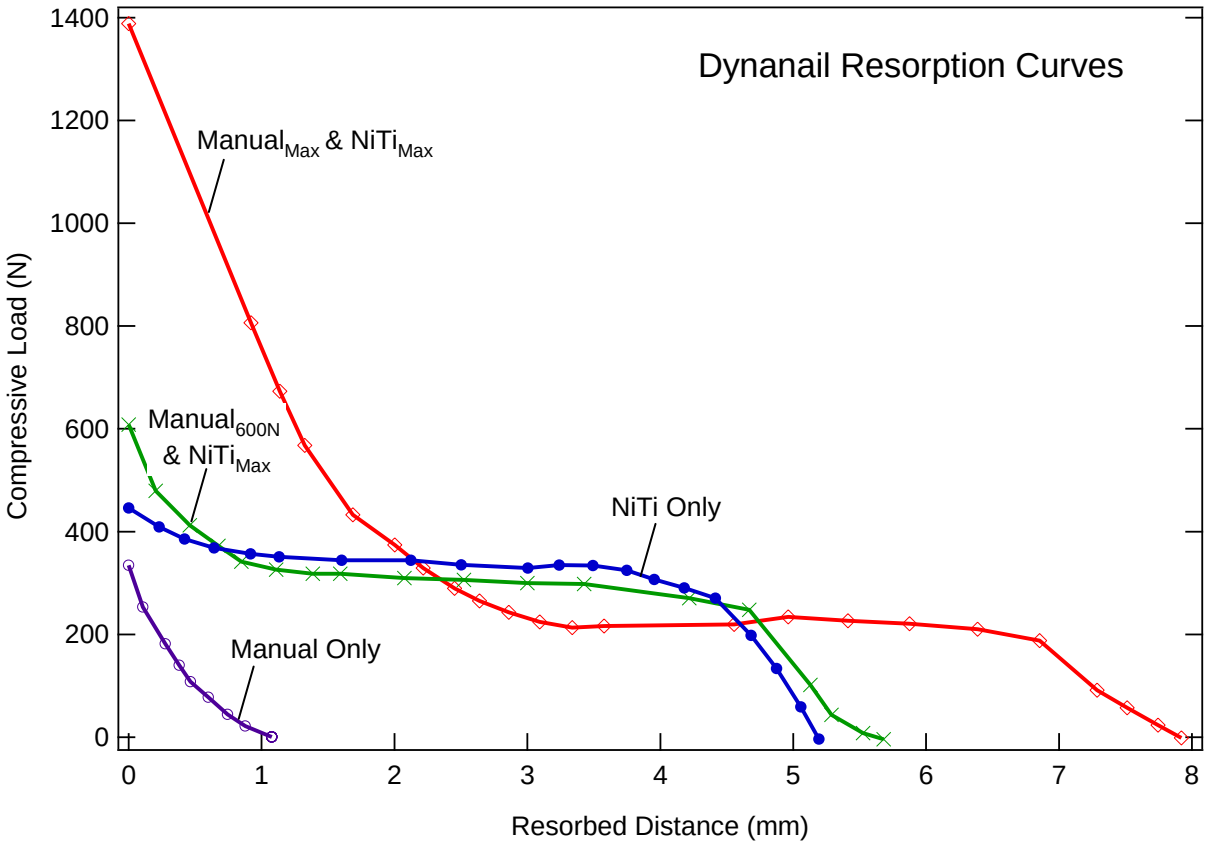

Figure 6. Resorption curves for all configurations of the Dynanail device.

Once the load equilibrates with the load sustained by the NiTi core, however, the curve plateaus, as seen in the case where only the dynamic element is loaded. The three configurations including NiTi activation demonstrate that the NiTi element maintains compression at a consistent load, but only once any additional compression has been lost. Also shown is a situation where only manual compression is employed for Dynanail. The resorption curve follows a similar trajectory to the Pantanail and Dynanail devices. It loses compression rapidly and reaches zero compression when only 1mm has been resorbed. When manual compression only is applied, all three of the nails lose 50% of their initial compression over only 0.3mm of resorption. The various loading scenarios for Dynanail are able to maintain

compression over a range of 1 to 8mm of resorption, where higher load levels in conjunction with the activation of the NiTi core maintain compression over the greatest resorptive distances.

3.2 Torsional Stability Curves

Figures 7, 8, and 9 show the torsional stability curves of Dynanail, Pantanail, and Versanail at different levels of initial compression. Each figure shows the average of all of the samples tested at the specified level of compression. In these cases, the individual resorption curves at each load level demonstrated consistency. The curves were normalized to zero and averaged, and the values of compression shown on the curve represent the average compression of each sample tested in that loading configuration. No data is shown in Figure 8 for the case of no load in the Pantanail device because there was high variability in the samples and an average value was not representative of the overall data.

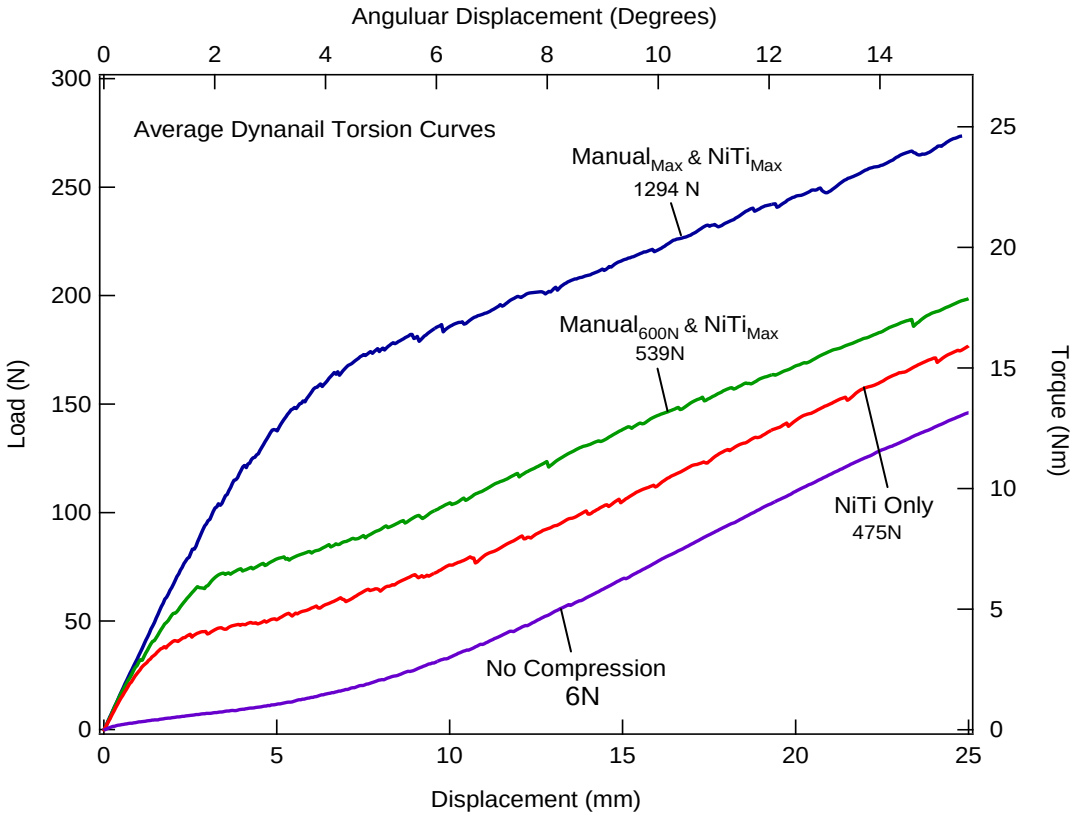

Figure 7. Average torsional stability curves for Dynanail at varying initial levels of compression.

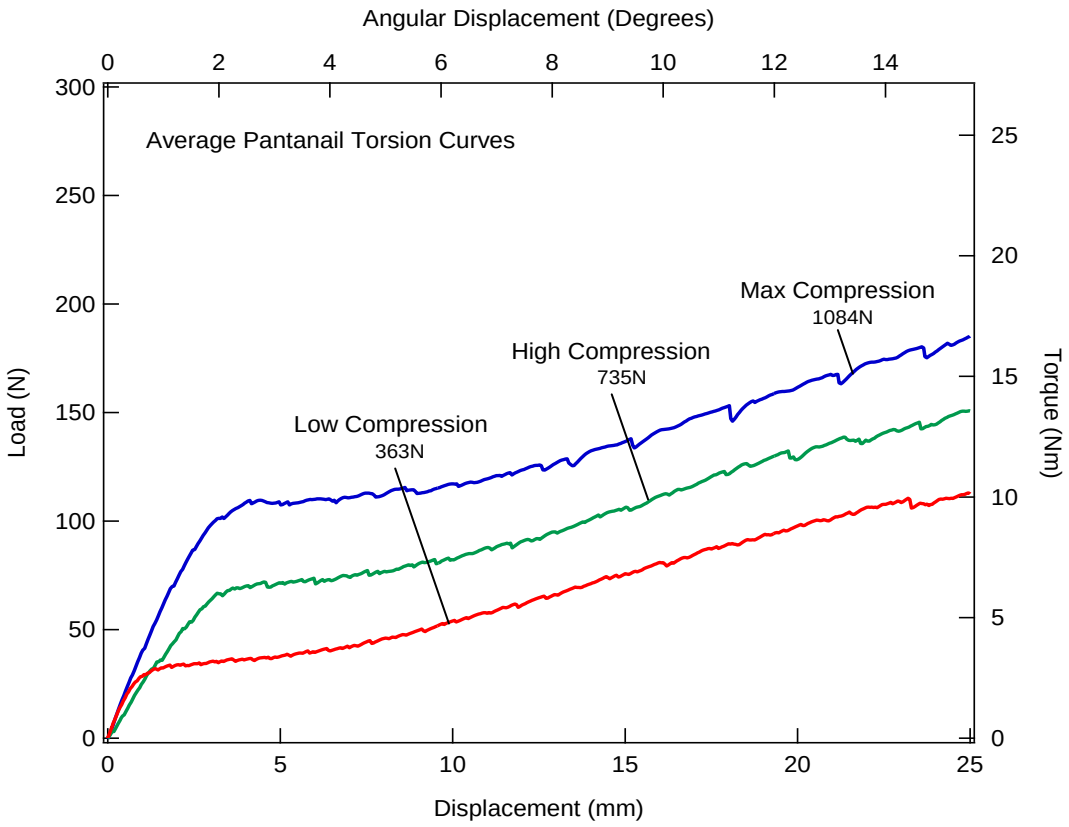

Figure 8. Average torsional stability curves for Pantanail at varying initial levels of compression.

Each figure demonstrates a definite trend towards increased torsional stability at higher compressive loads. Each of the curves is characterized by a relatively steep initial slope, demonstrating high torsional stiffness. This slope is interrupted by a break followed by a significantly decreased slope for the duration of the test. For each device, both the initial slope and the slope after the break have similar values regardless of the initial compressive load of the construct. This suggests that these values are a function of the test construct, nail geometry, or of the implantation parameters specific to that device, such as the size or orientation of the locking screws. While the slopes that define the curves are relatively uniform for each nail, the point at which the initial slope breaks varies significantly with the load level. The point where this break occurs is the only significant difference between the curves, indicating that it is related to compression.

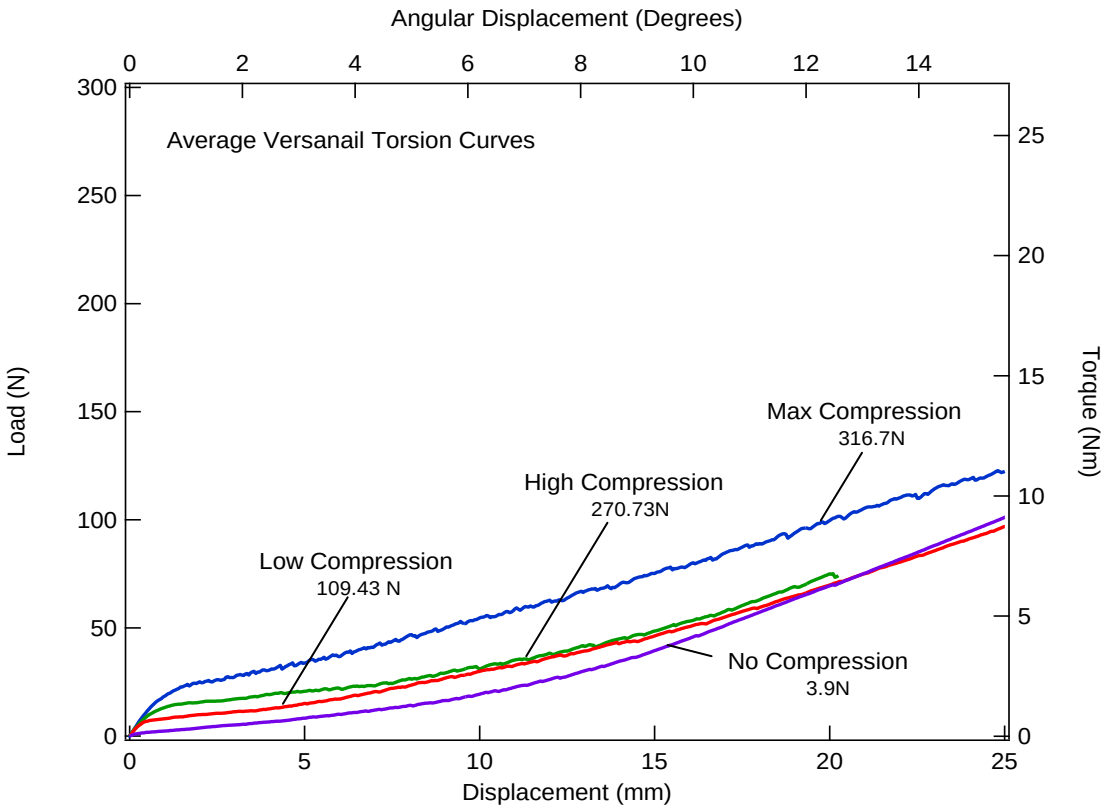

Figure 9. Average torsional stability curves for Versanail at varying initial levels of compression.

There was high consistency among the curves at a given load level in the majority of configurations tested. Though the actual compressive force varied with each implantation, the averages shown here are representative of all of the individual curves. This was not the case for the Pantanail device under no load, where the three curves failed to follow a similar trajectory. The data for the three curves of the Pantanail device under no compression is shown in Figure 10. These curves, though they vary, demonstrate the same thing as the average curves for the no load configurations in Dynanail and Versanail—in configurations with nominal or no compression, the torsional stability of the constructs are sacrificed. Figures 11 and 12 show the three curves for Dynanail and Versanail under no load, included for comparison.

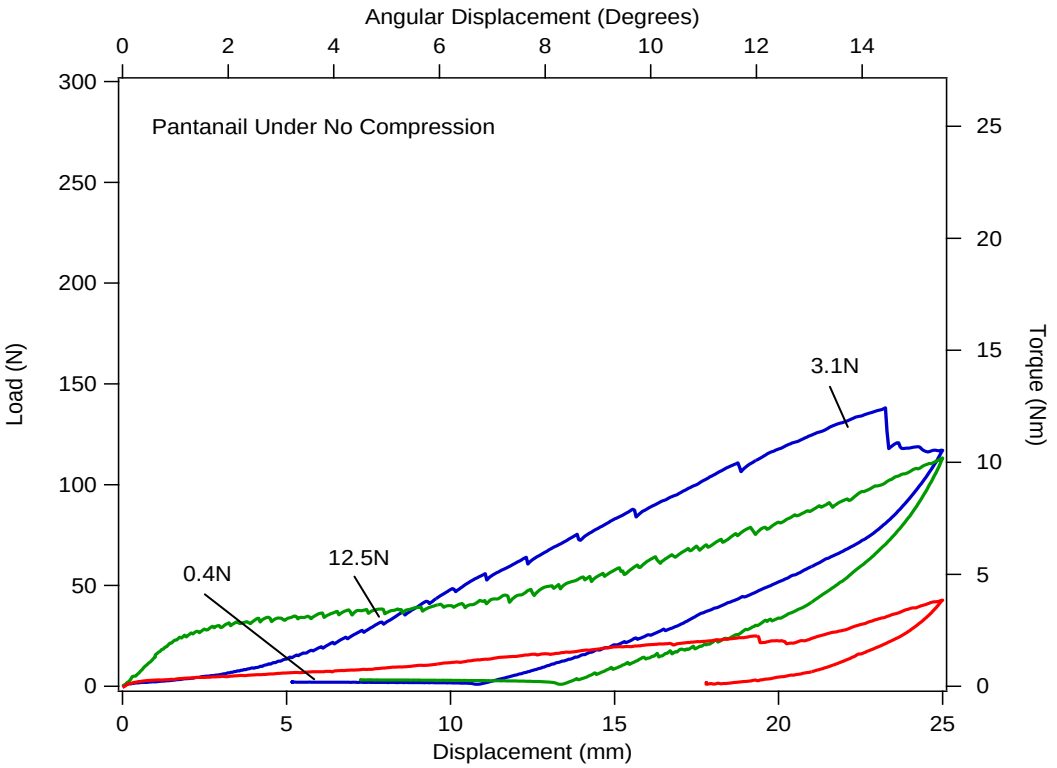

Figure 10. Torsional stability curves for each Pantanail sample tested at no load.

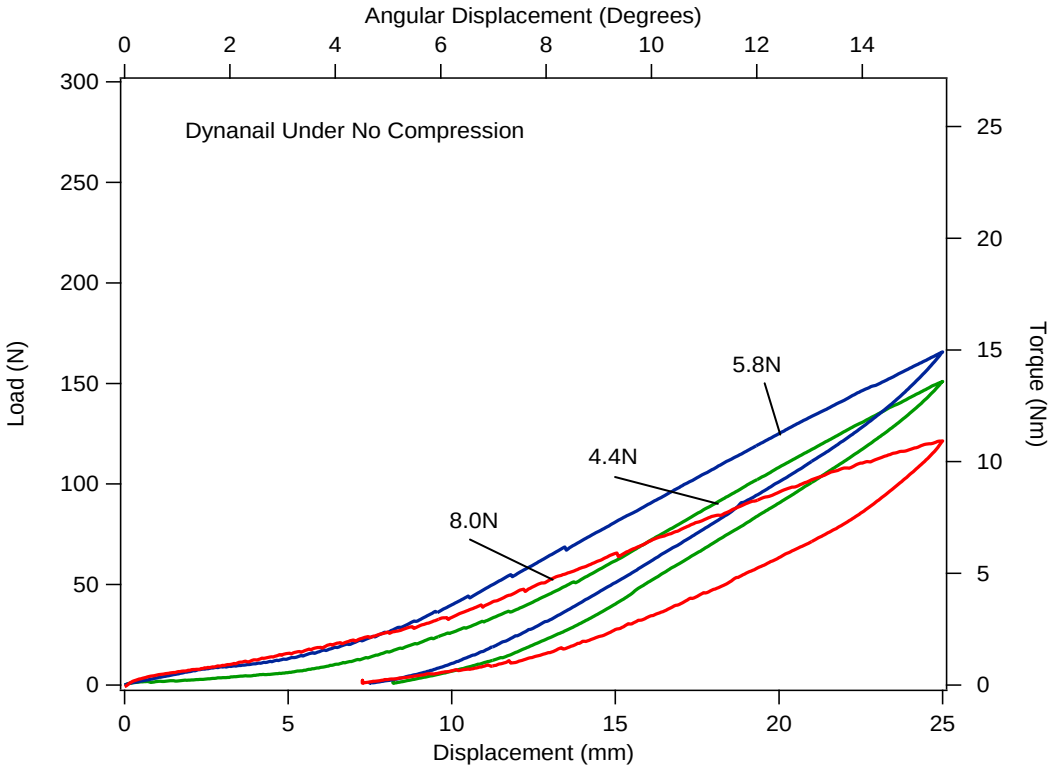

Figure 11. Torsional stability curves for each Dynanail sample tested at no load.

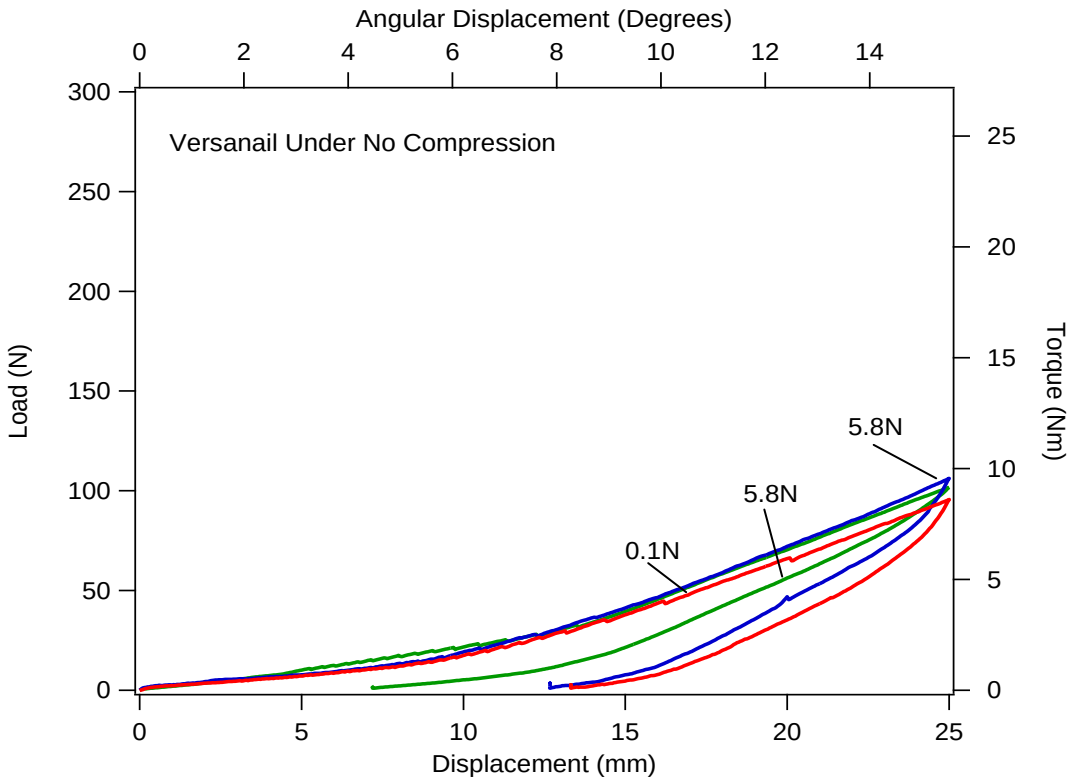

Figure 12. Torsional stability curves for each Versanail sample tested at no load.

A comparison of the torsional stability between the nails shows that Dynanail offers the greatest stability, while Pantanail offers higher torsional stability than Versanail. In each of its loading configurations, Versanail reaches the break point before 5 Newton-meters of torque is applied to the construct. Under little force, the high displacements of this construct indicate that is far less stable than the other two constructs. Pantanail and Dynanail have configurations that allow them to exceed 10 Newton-meters of torque before reaching their break. The ability to maintain high levels of stiffness with the application of increasing amounts of torque demonstrates that they are more stable constructs.

While it is apparent here that there are differences in the torsional stability of the devices, it is unclear from these curves whether it can be attributed to torsional stability differences in the device or if it is due primarily to the capacity of each device to maintain compressive force within the construct. Each device was tested in four configurations, but those

configurations were determined by the limits of the device and its instrumentation to apply and hold compression. The maximum compression achieved in each device for all samples tested is shown in Figure 13, where the error bars represent a 95% confidence interval. There is significant difference between the compression held in each of the three devices. Thus, it is likely that the most stable constructs result primarily from the higher compressive force.

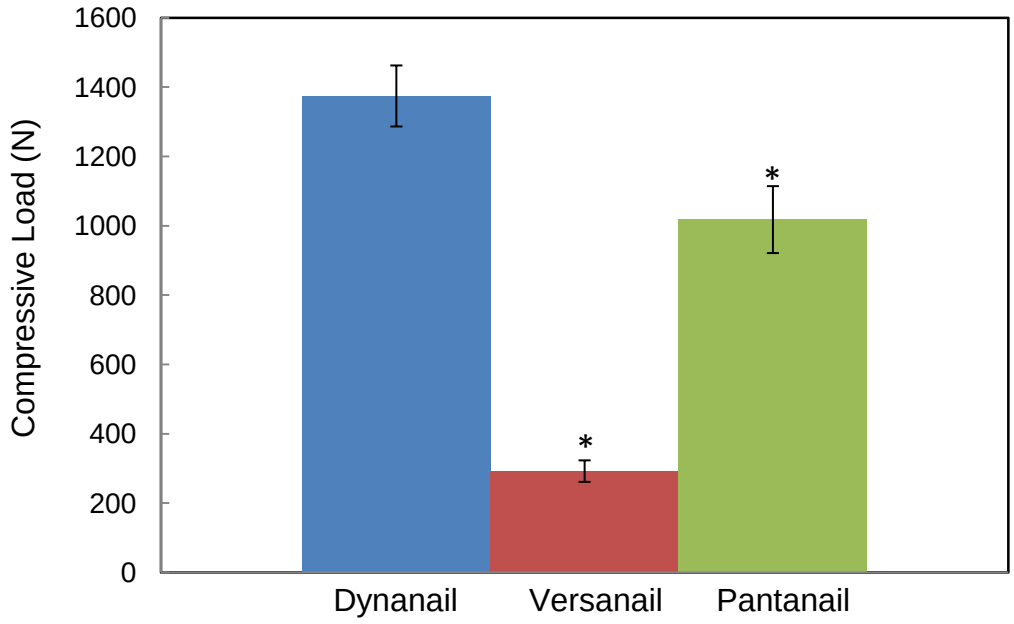

Figure 13. Compression maintained by each device after implantation in the maximum compression configuration. Error bars indicated 95% confidence interval.

A comparison of each device loaded at nearly equal loads is shown in Figure 14. This comparison shows that the nails behave similarly if the device is used to apply the same compression across the fusion site. The initial slope of the curve is similar between the three devices, suggesting that the factors dictating initial construct stiffness are either a function of the test setup or are similar between the nails. Most importantly, the curves break at approximately the same point in this figure. This indicates that if compression is held constant, there is no significant difference between the nails. A comparison of the nails tested under no load, as

shown in Figures 10, 11, and 12 also indicate that the torsional stability of the nails themselves, independent of compression, do not greatly vary. Thus, by first demonstrating that the capacity of the nails to maintain compression significantly differs, and then comparing the nails in two identical loading scenarios (no load and under the same load), it is evident that the compressive force the nail applies is driving the differences in torsional stability. It follows that the ability of Dynanail to exhibit increased stability is primarily a function of its capacity to generate and maintain higher compressive loads within the construct.

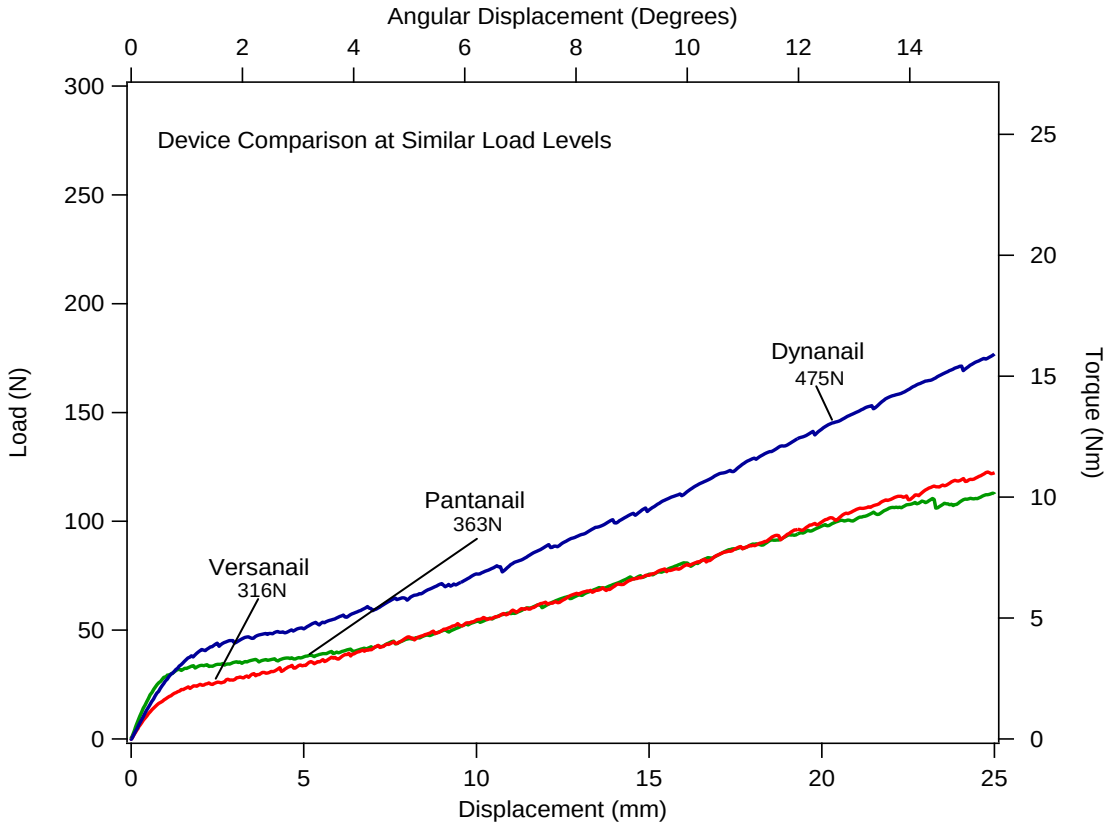

Figure 14. Comparison of torsional stability between three devices loaded to similar compressive loads.

CHAPTER 4

DISCUSSION

4.1 Relationship Between Compression and Torsional Stability

There is a clear relationship between the compressive force delivered by an IM nail and the torsional stability of the entire implant-bone construct. By breaking the torsional stability curves down into components and relating them directly to the compression of that sample, the effect of compression was further defined. Important aspects of the stability curve were deemed to be the initial slope, or stiffness, the displacement at the break point of the initial slope, the load at the break point, load at 8mm displacement (5° angular displacement), and load at 25mm (15.5° angular displacement). These points are delineated in Figure 15 below. For all samples tested, the values of these parts of the curve were extracted and correlated to the compression in the construct for that particular sample.

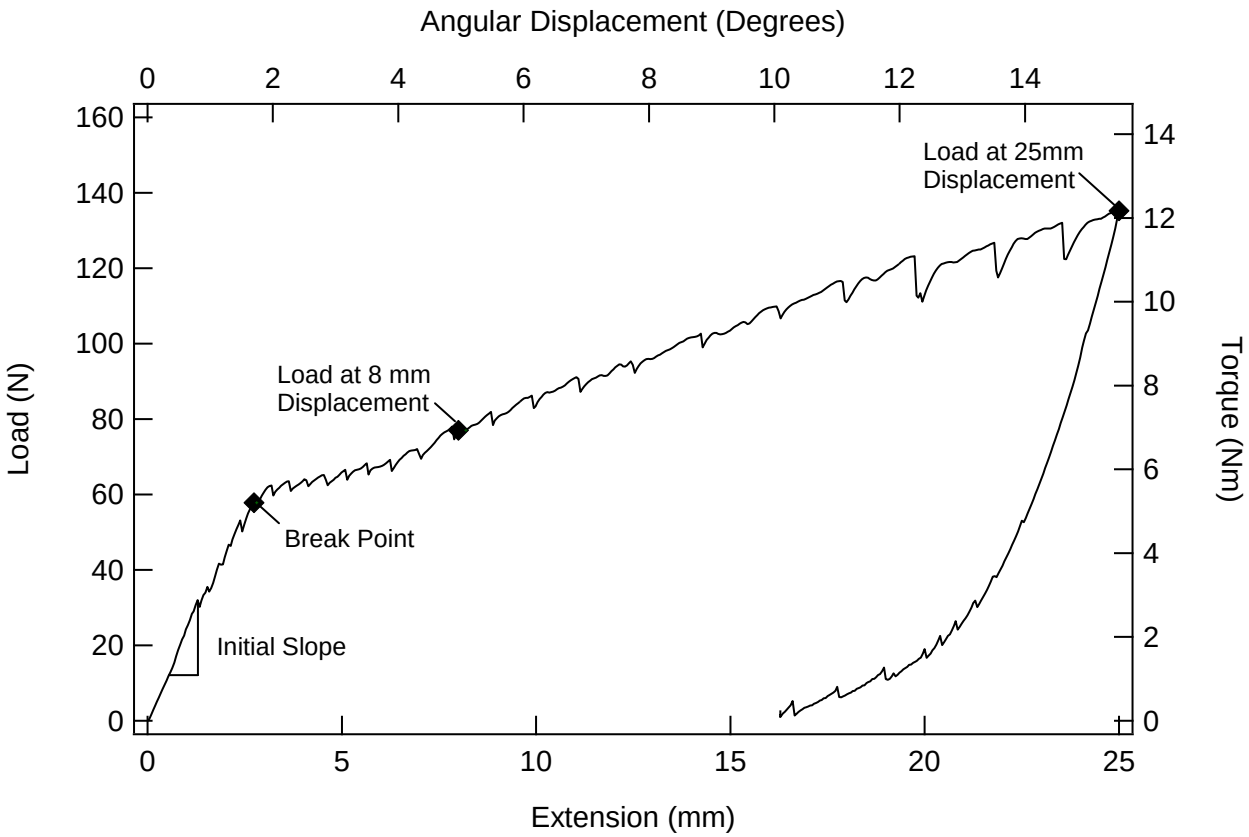

Figure 15. Characteristic torsional stability curve with defined aspects to relate to compression.

The correlation between the initial slope and the compressive load, shown in Figure 16, is positive, but not highly linear. The torsional stability curves themselves indicated that the initial slope was largely consistent, both within devices and among different devices. This figure highlights that while the gross variability of the initial slope is minor, the differences that do exist cannot be directly related to the increased compression in the construct.

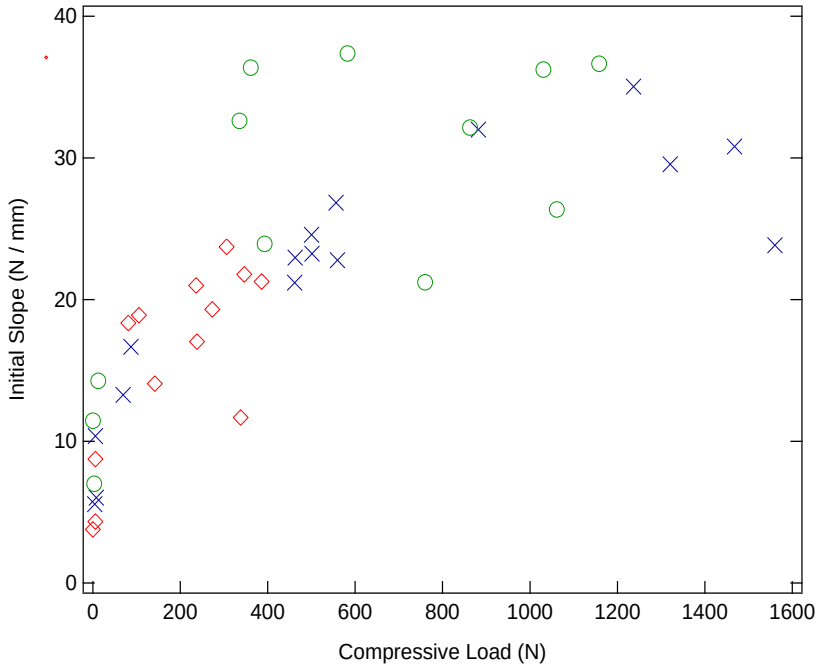

Figure 16. Correlation between the initial slope of the torsional stability curves and compressive load for ◊ Pantanail **o** Versanail **X** Dynanail.

Further, if the points with compressive values below 150 Newtons are eliminated, it is evident that the initial slope of each device, independent of compression, falls into a tight window. This is highlighted in Figure 17. The initial slope of Versanail ranges between 11 N/mm and 23 N/mm. Pantanail has a range between 21 and 37 N/mm while Dynanail ranges from 21 to 35 N/mm. This data reinforces the fact that the initial slope of the torsional stability curve is most likely related to factors inherent to the construct. The addition of compression may play a role in altering the initial torsional stiffness, but the slightly positive correlation is not strong enough to suggest that compression alone dictates the initial slope of the curve.

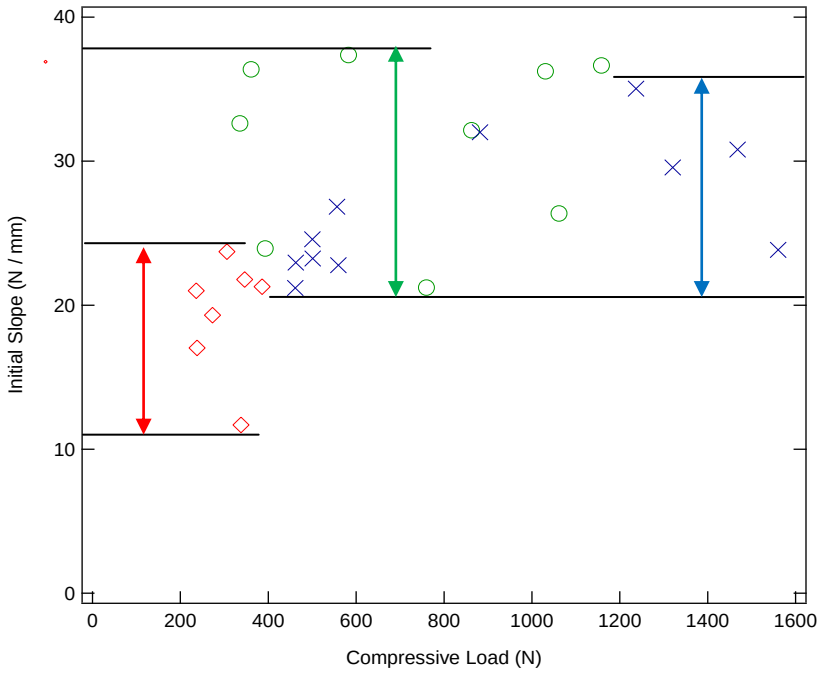

Figure 17. Range of values of initial slope of the torsional stability curves for each nail. ◊ Pantanail **o** Versanail **X** Dynanail.

Figure 18 and 19 show the relationship between the displacement and load at the break point of the curve, respectively. These plots show a strong positive correlation between the compressive load and the point at which the stability curve breaks to a less steep slope. Because the initial slope was found to vary only slightly between devices and different compressive loads, it follows that both the load and displacement at the break are highly correlated to the initial compressive load.

Further correlations were drawn between the load at 8 and 25 mm of extension and the initial compressive load of each sample. The load at 8 mm, shown in Figure 20, demonstrates a strong positive correlation with the compressive load. The load at 25 mm, however, has significantly more scatter, shown in Figure 21. While there is a slightly positive trend, there is no strong indication that compression controls the load at 25 mm of the stability curve.

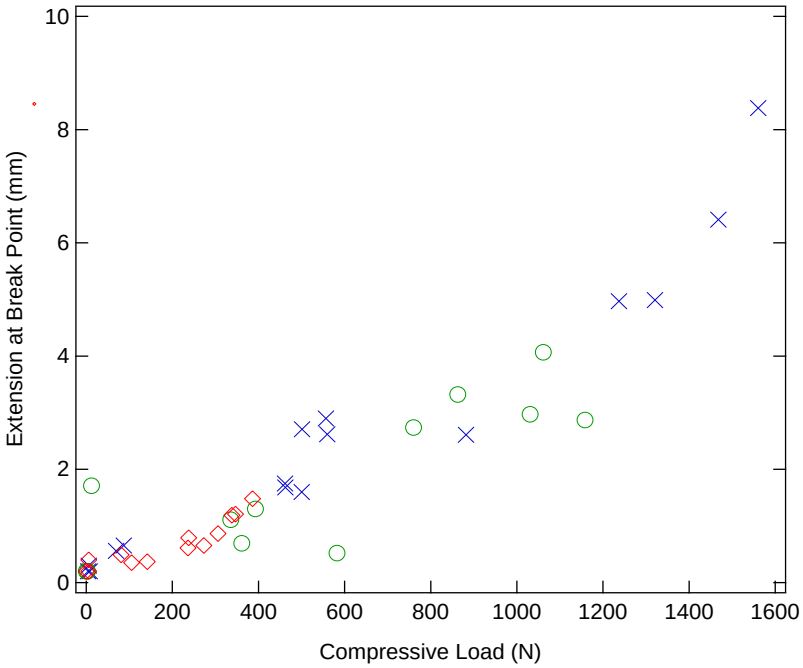

Figure 18. Correlation between the displacement at the break point of the torsional stability curves and compressive load for ◊ Pantanail **o** Versanail **X** Dynanail.

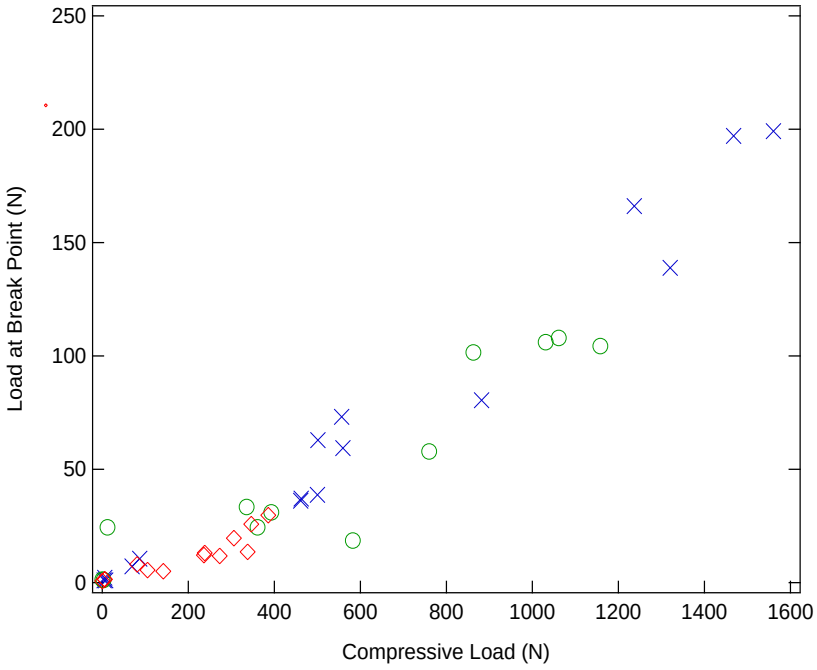

Figure 19. Correlation between the load at the break point of the torsional stability curves and compressive load for ◊ Pantanail **o** Versanail **X** Dynanail.

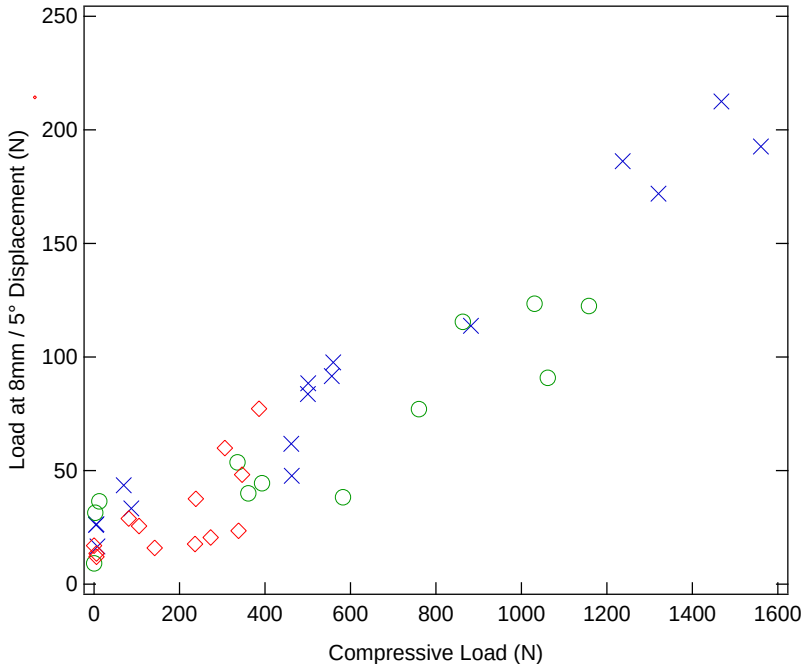

Figure 20. Correlation between the load at 8mm (5°) displacement of the torsional stability curves and compressive load for: ◊ Pantanail **o** Versanail **X** Dynanail.

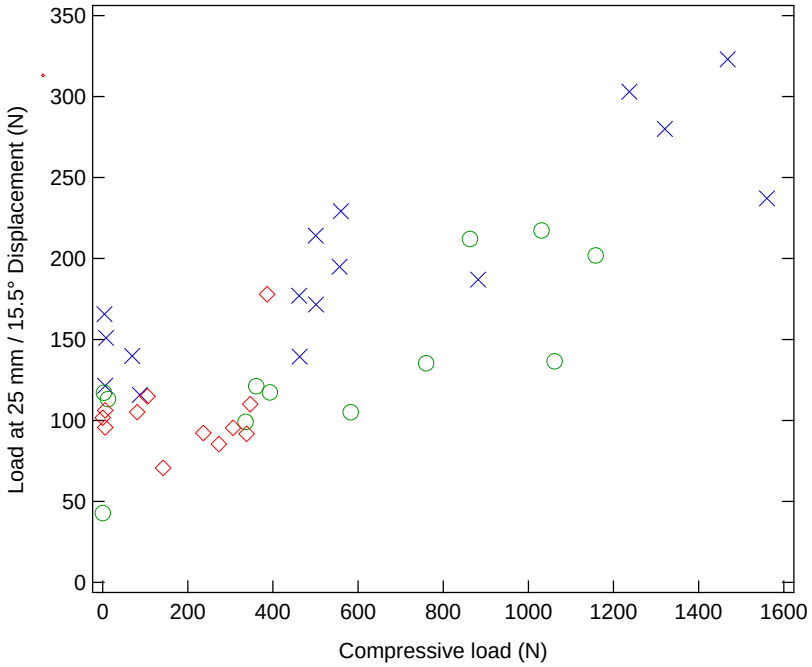

Figure 21. Correlation between the load at 25mm (15.5°) displacement of the torsional stability curves and compressive load for: ◊ Pantanail **o** Versanail **X** Dynanail.

The combination of these relationships provides insight into which aspects of the stability curve are affected by the application of compression. The coefficient of determination, R^2, was calculated for each of these correlations, both for the individual nail and the data as a whole. Those values, shown in Table 4, confirm that the highest correlations are found between compression and the load and displacement at the break point as well as the load at 8mm.

.

Table 4. Strength of correlations (R^2 value) between defined variables and construct compression.

Variable	Versanail	Pantanail	Dynanail	Overall
Load at 8mm Ext	0.4789	0.8327	0.9612	0.8837
Load at 25mm Ext	0.0909	0.6145	0.7606	0.6301
Initial Slope	0.5389	0.4677	0.6634	0.5464
Break Point Ext	0.7893	0.7018	0.9297	0.8581
Break Point Load	0.7988	0.8616	0.96	0.9207

The strongest correlations occur at and near the break point. Because most nails with low compression break before 8mm and those with higher compression break near 8 mm, this point of the curve is also highly correlated to the initial compressive load. The load at 25mm, however, is poorly correlated. This suggests that, like the initial slope, the slope of the stability curve after the break point is not affected by the compression in the construct. The variation seen in the slope of the curve after the break is high; some devices were characterized by a constant low slope while other had low slopes after the break that turned up at higher degrees of displacement. Ultimately, once the static friction preventing the respective movement of the sawbone at the joint has been overcome, the stiffness of the construct isn't well correlated to compression. The point where the friction between the joint surfaces is broken, however, does appear to be a function of the compressive load. At the point of the break, where the static friction is being overcome, the compressive force is the normal force between the sawbone surfaces. As such, that compressive force dictates where the break point will be. After static

friction has been overcome, the resulting movement is a function of both kinetic friction at the joint surfaces and locking screw interaction with the nails and bone. Factors potentially affecting the stability curve after the break point likely include the length, orientation, or geometry of the locking screws.

Figure 22 summarizes the points of the curve analyzed, including those that were determined to be significantly impacted by compression as well as those that are most affected by other variables.

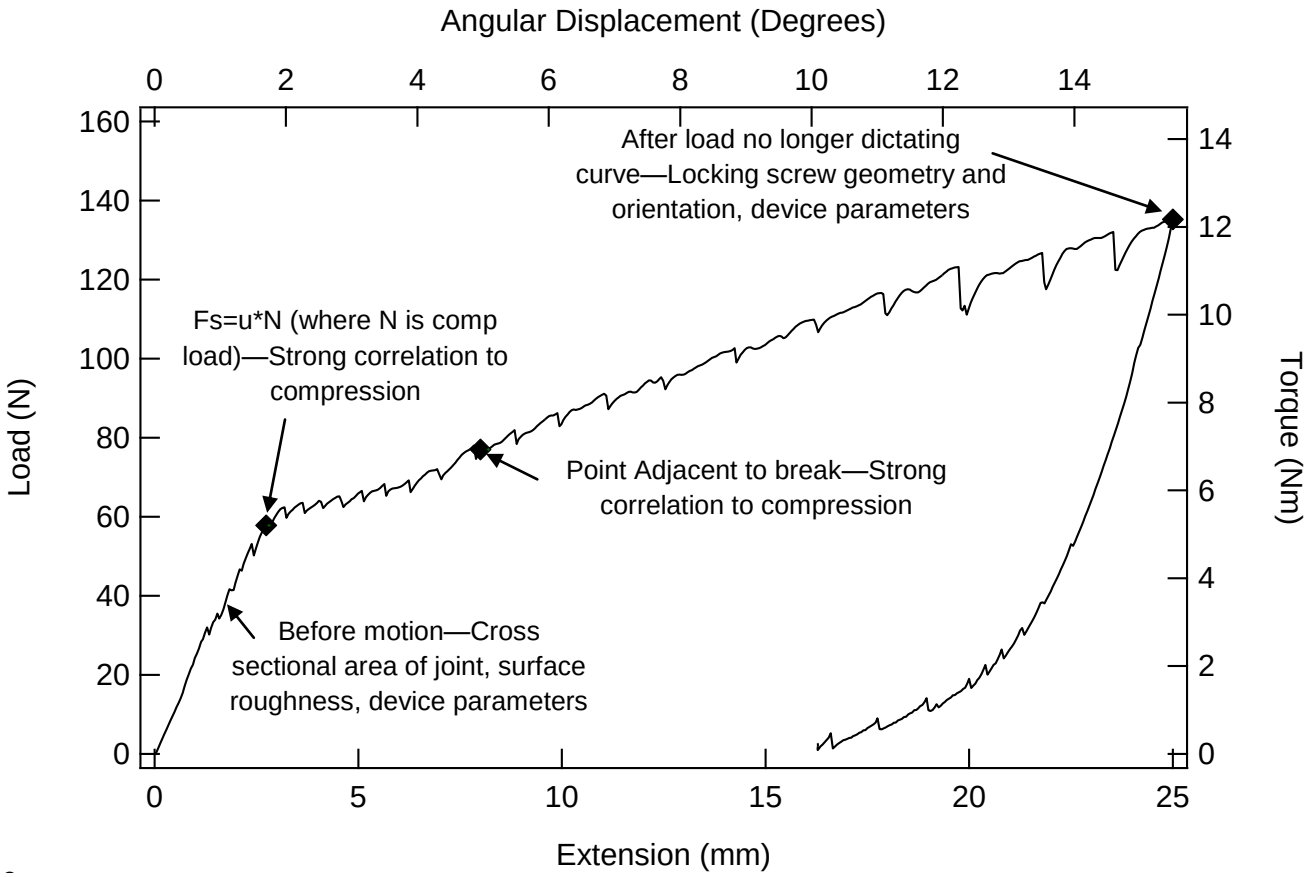

Figure 22. Summary of torsional stability curve.

4.2 Construct Stability Over Simulated Resorption

The previous data establish the correlation between compression and torsional stability in a model of ankle arthrodesis. In essence, the torsional stability of a device will depend on the limitations of that device to maintain compressive force. At the time of implantation, the device with the highest level of compression will typically be the most stable. Figure 23 demonstrates the torsional stability of Dynanail, Pantanail, and Versanail upon implantation in their maximum load configurations.

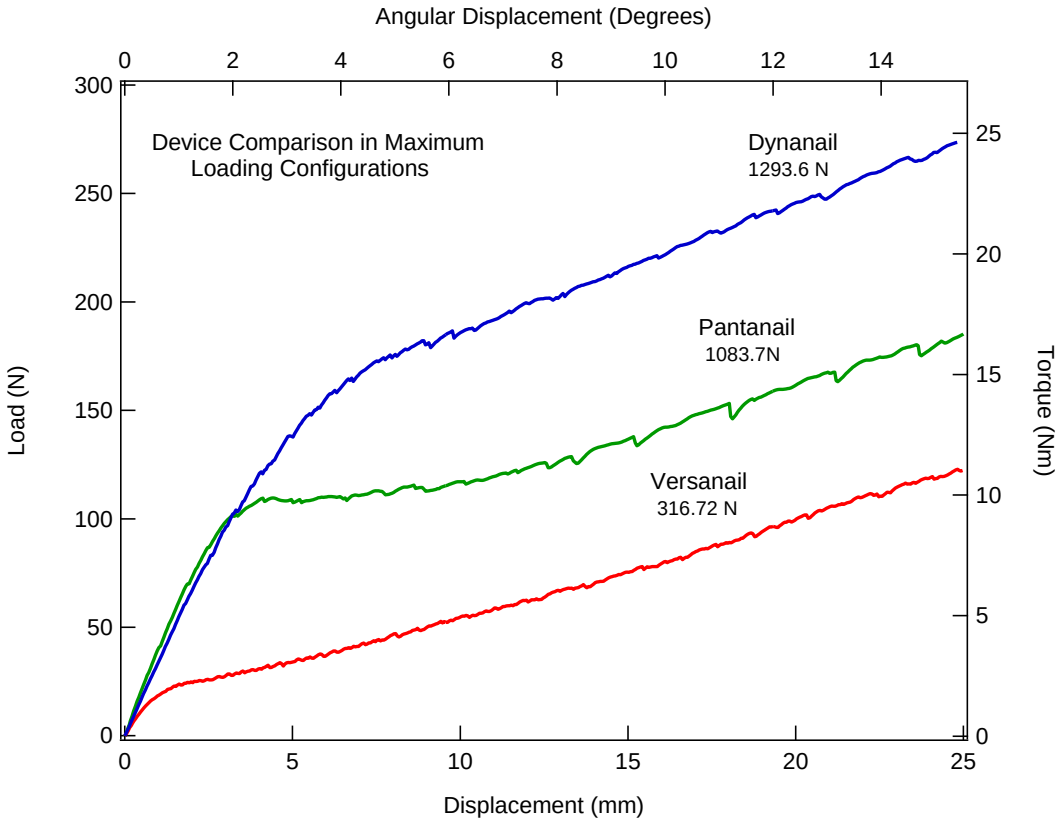

Figure 23. Torsional stability curves of the three devices in their maximum compression configurations.

This level of torsional stability will only be maintained as long as that level of compression is maintained. Because bone healing is known to cause bone resorption, the resorption model presented here provides a means of estimating what happens to the torsional stability of the construct over time. Table 5 presents the range of loads that were maintained by

the nails at various levels of resorption. Linear interpolation was used to predict the loads when a measurement wasn't taken at the specific resorption value noted.

Table 5. Compressive load maintained at various levels of resorption.

Resorption	Versanail	Pantanail	Dynanail
0.25 mm	107-117 N	439-691 N	1117-1230 N
0.5 mm	2-13 N	16-367 N	787-1072 N
1 mm	0 N	0-21 N	561- 757 N
4 mm	0 N	0 N	217-258 N

The loss of compression that occurs over 0.25mm of resorption varies significantly between the devices. Figure 24 illustrates these differences, where the bars represent the maximum load and the shaded portion of the maximum compression bar represents the average compression maintained by each device after 0.25mm of resorption. Further losses in compression occur as the resorbed distance increases, but the most dramatic losses occur immediately, which is evident in this figure.

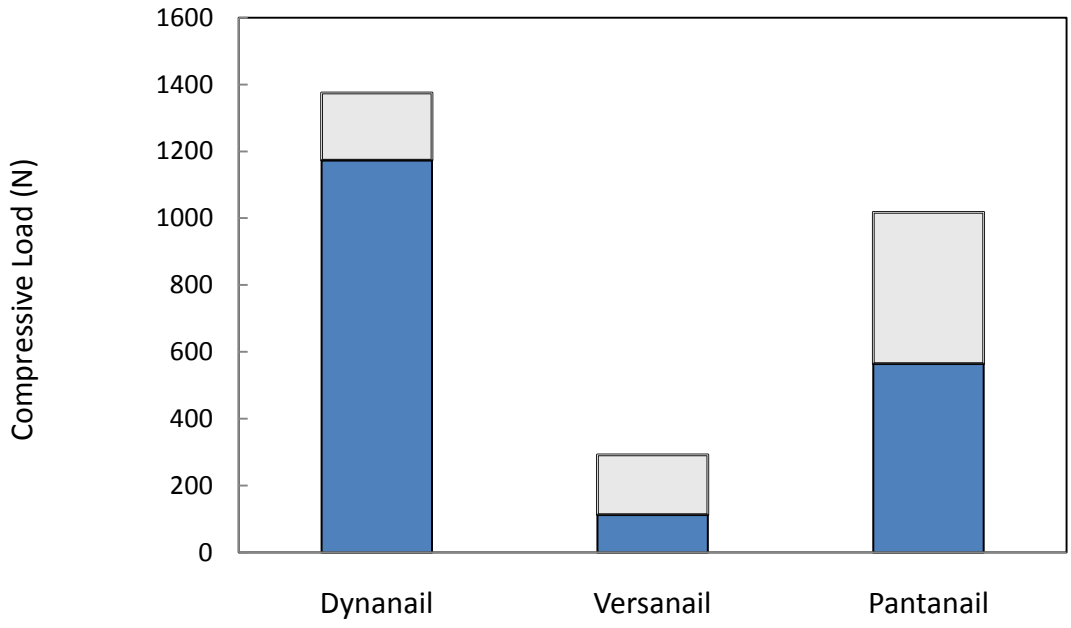

Figure 24. Amount of initial compression maintained by each device after 0.25 mm of resorption.

At each level of resorption— 0.25, 0.5, 1, and 4 mm—a torsional stability curve for each device is presented. The particular curve chosen is based on the initial compression of the sample, where the compressive value either fits within or is near the load range specified in the table above. Figure 25 illustrates the torsional stability of the three devices after 0.25mm of resorption has taken place.

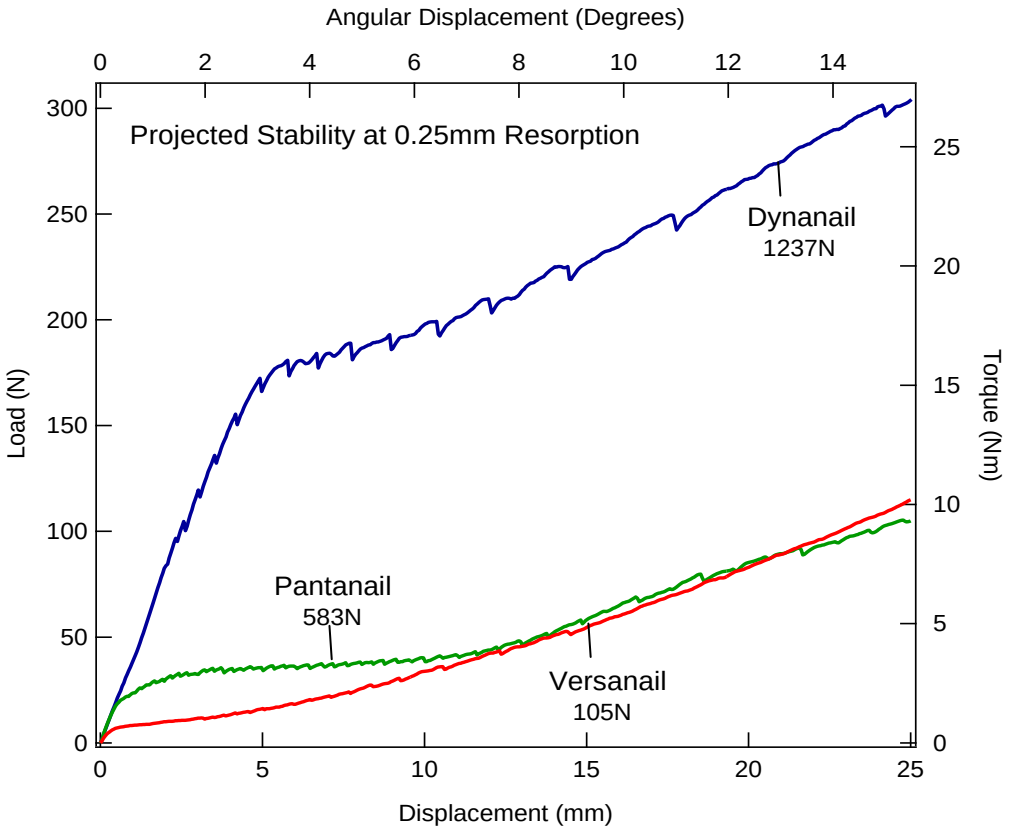

Figure 25. Torsional stability curves of the three devices at loads representing the constructs after 0.25mm of resorption.

The graph demonstrates how significantly a small amount of resorption can affect the stability of the implant-bone construct. The nominal load maintained by Versanail is ineffective in resisting torque. Pantanail maintains a higher load and some stability of the construct, but Dynanail's load reduced only slightly, making it by far the most stable construct at 0.25mm resorption.

Figures 26**,** 27, and 28 show the torsional stability curves representing loads at 0.5 mm, 1 mm, and 4mm of bone resorption, respectively.

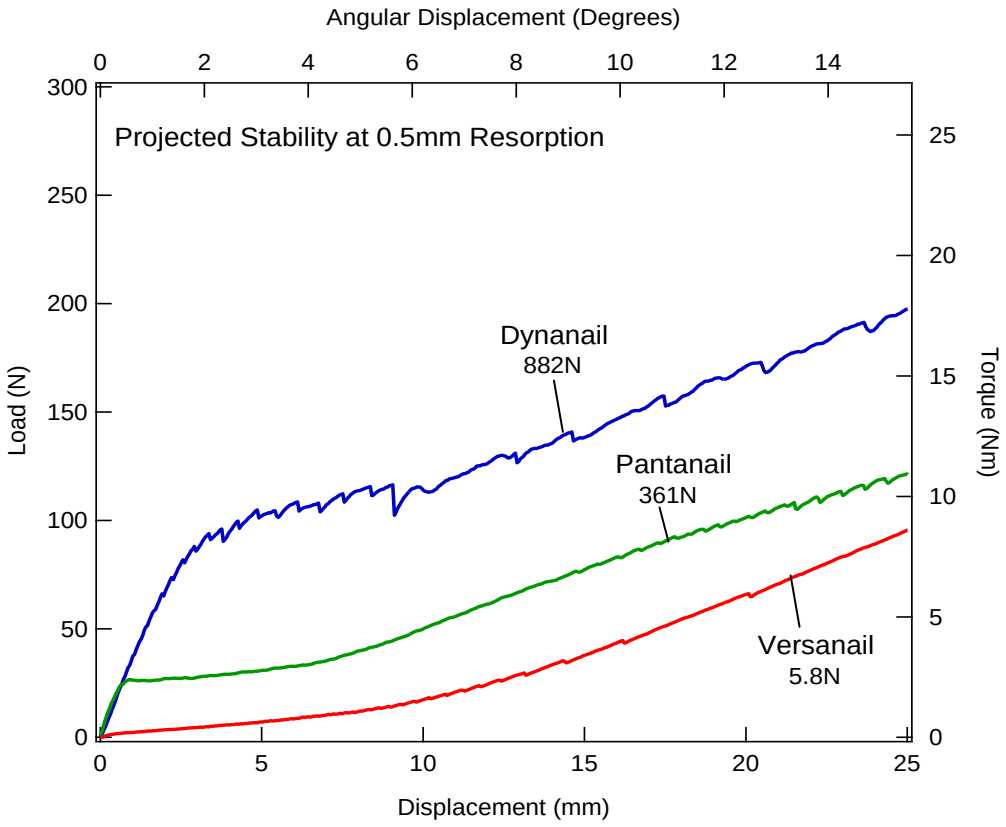

Figure 26. Torsional stability curves of the three devices at loads representing the constructs after 0.5mm of resorption.

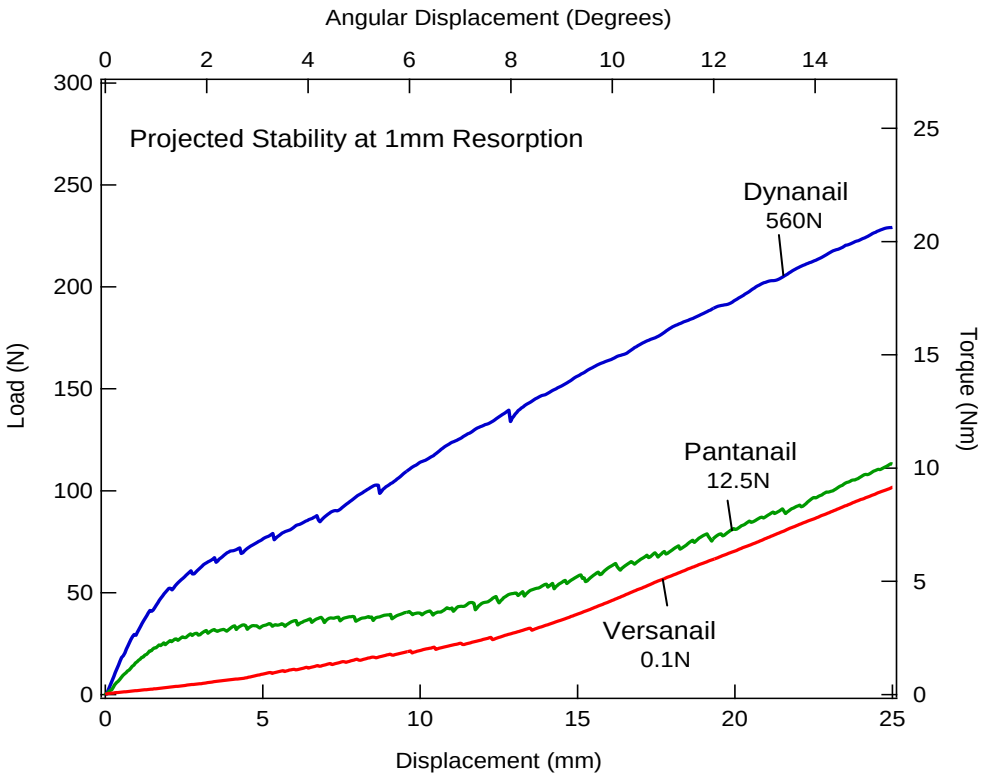

Figure 27. Torsional stability curves of the three devices at loads representing the constructs after 1mm of resorption.

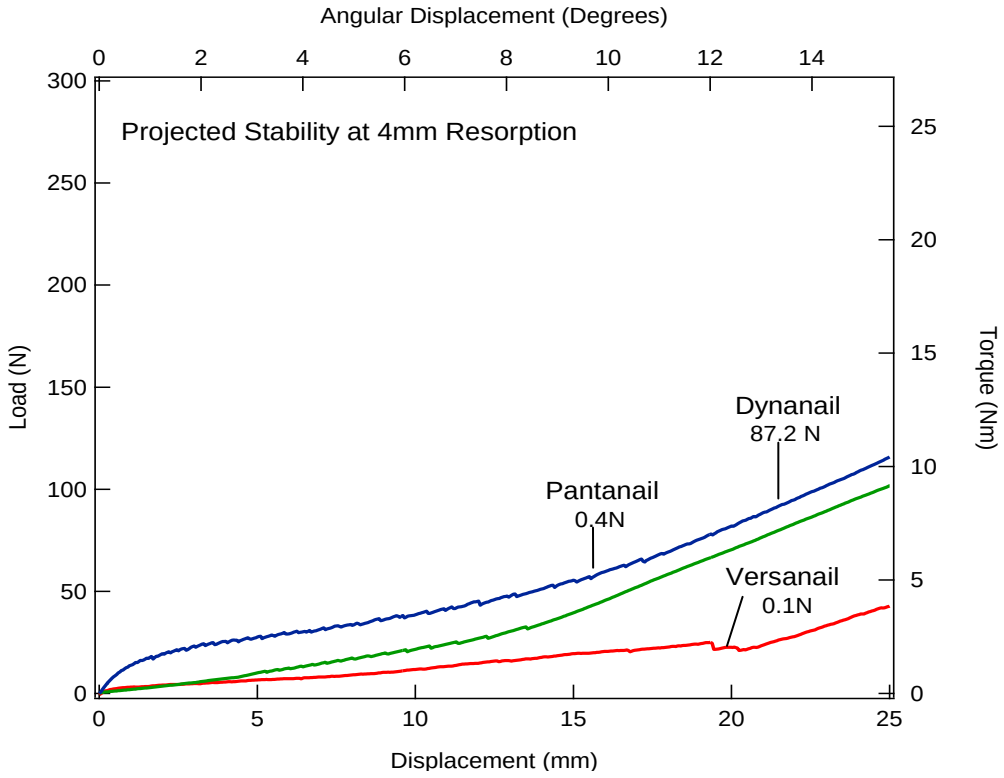

Figure 28. Torsional stability curves of the three devices at loads representing the constructs after 4mm of resorption.

These curves provide insight into the substantial loss of stability that occurs in an ankle arthrodesis device over the course of bone healing. At 0.5 mm of resorption, Versanail has lost virtually all compression and the compression maintained by Pantanail offers decreased stability, where only 2.5 Newton-meters of torque can be sustained before high levels of displacement occur. By 1 mm of resorption, neither Pantanail nor Versanail are offering any stability to the construct in torsion. Dynanail has lost some compression but is still able to withstand approximately 5 Newton-meters of torque before its break point. By 4 mm of resorption, Dynanail has lost more compressive force, but still provides some stability to the construct.

It is relevant to ask whether there is necessity for compression to be maintained over 4mm of resorption. In a study performed my Pelton of dynamically locking nails, the amount of movement of the dynamic screw in the locking slot was measured. This movement was the result of bone resorption and impaction, as the dynamic mechanism allows for load sharing and earlier weight bearing. The average movement of the nail was assessed to be 2.3 mm [3]. The same study made note of one patient in whom the impaction exceeded the 5 mm movement allowed by the dynamic locking slot. In this scenario, the construct would be actively holding the ends of the bones apart; surgery was performed to remove the screw to allow the bone to fuse. This data both confirms that significant resorption does occur during the bone fusion process and highlights shortcomings of the currently available devices. Not only is the dynamically locking feature limited to 5 mm of bone impaction or resorption, but the result of exceeding that pre-determined resorption level is a second surgery and screw removal. Once the dynamic locking screw is removed, the intramedullary device will offer no torsional stability. Current devices rely on the increased strength of the developing callus to resist deformation, but the Dynanail device would provide added support to the construct throughout bone healing. This additional stability, in conjunction with the maintenance of joint congruency, could be the

difference between successful bone fusion and repeated operations in the 22% of ankle arthrodesis procedures that fail.

CHAPTER 5

CONCLUSIONS

The data presented in this work suggest that it is possible to improve current ankle arthrodesis technology by incorporating a NiTi compressive element into the body of a traditional nail. Decreased compression in the bone-implant construct was shown to affect the point at which the initial stiffness of the construct is lost under applied torque. The ability to sustain higher torques could potentially be the difference between interfragmentary micro-motion, which is beneficial to bone healing, and macro-motion, which can increase the bone strains beyond the effective healing limits. Under conditions of rigid immobilization, there might not be function in resisting torques that will never be applied to the construct. Current devices, however, are promoting earlier weight bearing, making the ability of the construct to withstand the outside forces it's subjected to important in enabling healing.

By relating the known effect of resorption to a decrease in compressive load with the resorption model, this study demonstrated the effects of resorption on the torsional stability of a bone-implant construct. The compression offered in current devices is applied at the time of implantation, but lost once any bone resorption takes place. This effectively resulted in little to no torsional stability over time. Dynanail, however, demonstrated some torsional resistance even at 4 mm of resorption. The ability of the construct to withstand torsional forces throughout healing is likely to enhance the bone remodeling process.

This study demonstrates the effectiveness of compression in increasing torsional stability and the results of resorption on torsional stability of the construct. The incorporation of a NiTi compressive element in the Dynanail device was able to provide *sustained compression* that increased the torsional stability of the construct over time. The use of such NiTi components could be beneficial in other applications, including hip fracture, humerus fracture, or other sites of arthrodesis.

APPENDIX A

NiTi APPLICATION IN HIP FRACTURE

Hip fracture is a significant problem in the United States, with upwards of 250,000 incidents occurring annually in patients over 65 years of age [25]. In 1990, there were an estimated 12.6 million hip fractures worldwide, 917,000, or 73% of which, belonged to females [26]. Women represent the vast majority of hip fracture cases, which are primarily incurred by a sideways fall onto the hip. While elderly women are at the greatest risk of sustaining hip fracture, other risk factors include malnutrition, decreased physical activity, balance problems, and osteoporosis [27]. As the aging population continues to grow, worldwide projections for instances of hip fracture are expected to double to 2.6 million by year 2025.

More alarming than the sheer magnitude of occurrence, however, is the poor prognosis that many patients face. Mortality at one year has been reported to be 33% [28], where the 5-year survival rate for hip fracture patients is only 41% [29]. Immediately after surgery, patients face hospitalization time that can average as many as 30 days [30]. After being released from the hospital, up to 42% of people who lived independently prior to their fracture are confined to a nursing home, where they may spend a full year or more [31]. As many of 17% of hip fracture patients spend the duration of their lives in a nursing home [32]. The extensive care required for these patients contributes to the extraordinary expense associated with hip fracture. Hip fracture costs have been estimated at $81,300 per patient, approximately half of which was related to nursing facility expenses [32]. The immense cost that this amounts to is most significant in comparison to other osteoporosis-related fractures. Of all health care expenditures attributed to osteoporotic fractures, 63%, a total of $8.68 billion dollars, goes towards hip fractures alone [33].

The overwhelming incidence and cost of hip fracture demand an equally large effort to treat the problem. Most often, hip fractures are treated surgically, where the type of fixation is

dependent upon the location and type of fracture. Though many classification systems exist, hip fractures can typically first be divided into neck fracture, intertrochanteric fracture, and subtrochanteric fracture. Femoral neck fractures are often treated with hip pinning, where the primary operative function is to maintain union among the fracture fragments and additional structural support of the construct isn't necessary. Hemi- or total arthroplasty can be done in cases of extreme osteoporosis or in revision surgery where the femoral head has been destructed by previous screws [34]. Intertrochanteric fractures, which account for 50% of all hip fractures, are more demanding to treat because they often rely on the lateral support a device can provide to offer a stable healing environment [35]. In these cases, hip screws—in a side plate or intramedullary nail configuration—are often employed. In these devices, the hip is instrumented with a rigid intramedullary or side plate device which a large cancellous screw passes through, engaging the fragmented femoral head. The screw acts to maintain union among the fracture fragments while the rod or sideplate provides the lateral and structural support necessary.

The side plate was developed in the 1950s as a means of advancing the nail-plate systems that were found, at the time, to have benefits over non-surgical treatment. The failures of the nail-plate system, including protrusion of the nail into the hip joint, cutting upwards through the cancellous bone of the femoral neck, and bending and breaking at the angle, were largely attributed to the rigidity of the device [36]. Here, nail placement became a catch-22; if the screw wasn't placed far enough into the femoral head to engage solid cortical bone, it would act as a hinge in the soft trabecular bone, allowing the screw to cut upwards. But if the screw was placed far enough initially, the process of bone resorption during the dynamic bone healing process could drive the screw through the femoral neck and into the joint capsule. The solution was to introduce a sliding capacity into the device—a side plate with was fixed to the lateral diaphysis with an angled barrel through with the cancellous screw was able to slide. Sliding introduced a dynamic aspect to a still rigid structure, allowing the screw to engage the femoral

head without creating a distinct separation between fracture components during bone healing. Additionally, sliding allowed for impaction of fracture fragments which serves to stimulate callus formation, thereby accelerating bone healing [36].

While sideplate devices have been successfully employed since their advent and are still considered a gold standard in hip fracture fixation, they can experience failure rates as high as 23% [37]. They can fail via separation of components in a highly comminuted fracture or through a loss of sliding action that results in the same failures seen with rigid devices—cutout of the femoral head. In the 1990s, the shortcomings of the sliding hip screw were addressed with a new device—the intramedullary nail. The IM nail was meant to improve patient outcome by offering improved fixation biomechanics, a minimally invasive insertion, and shorter time to weight bearing, while maintaining the same sliding advantages of the side plate devices [38]. Fracture biomechanics were expected to improve because the intramedullary placement of the load bearing mechanism allows the transmission of weight down the shaft of the femur, where the side plate devices sit laterally to the load line. This medialization of the femoral component of the device would also decrease the lever arm of the bending force, hopefully leading to fewer device failures [39].

Since both the intramedullary and side plate devices have been on the market, numerous biomechanical and clinical studies have attempted to determine which is the superior means of fixation. While findings have varied significantly among different studies, the foreseen benefits of a semi-closed procedure in the intramedullary devices have been stymied by the fact that is a more technically demanding procedure with more challenging placement of the lag screw [40]. As such, the surgical time and blood loss are not consistently reduced with the use of an intramedullary device. The difficulty in placing the lag screw in the IM nail's closed procedure leads to a similar or increased occurrence of failure via lag screw cutout in IM nails over side plate devices [36]. Ultimately, findings have been unable to point to a clearly superior means of fixation [41], and the anticipated benefits of the IM device have not been fully realized.

While no conclusive studies have been able to indicate that intramedullary fixation is superior to side plate fixation, trends in device use indicate that the market is leaning more towards the use of intramedullary nails for hip fracture fixation [42]. This could be attributed to the ability to use IM devices more successfully in subtrochanteric and unstable fractures, where the intramedullary location of the femoral component allows for structural support the lateral side plate cannot offer [40]. Regardless of the reason, the continued and increased used of IM devices provides incentive to improve current devices. In doing so, identifying and understanding the primary causes of failure is important.

Intramedullary devices fail, primarily, in one of two ways. The femoral shaft can fracture at the tip of the nail, where a stress concentration is introduced via the abrupt change in stiffness between the supported and non-supported femur. These failures are specific to IM devices [43], and can occur in 8-17% of cases [43-45]. The most common form of failure, however, is cutout of the lag screw from the femoral head [45-47]. Cutout, which occurs when the lag screw migrates far enough in the femoral head to puncture the cortical layer superiorly and enter into joint capsule, has been identified as a cause of failure in 5-23% of cases [40, 43, 47-48]. Many factors have been suggested to be significant in causing or preventing cutout, the most widely recognized of which include bone quality [49], lag screw placement (often noted as the tip-apex distance) [40, 45, 49-51], and anatomical reduction [45, 47]. Here, bone quality is an important issue as it relates directly to the fixation strength of the lag screw in the femoral head. While important, it is patient-specific and independent of device design. Similarly, many studies focus on the importance of achieving a tip-apex distance (placement within the femoral head) that is within 25mm of the apex of the femoral head (where 25mm is a summation of the lateral and frontal screw position). It can be deduced, however, that this position is desirable primarily to ensure that the lag screw engages in the most dense bone possible without being placed though the cortical layer. As such, position is important, but can be considered a function of bone quality. Anatomical reduction, on the other hand, indicates that maintaining

alignment of fracture pieces is important. Reduction is a surgeon-dependent practice that is, currently, not reliant upon device design. Thus, while it would be difficult to directly affect reduction with a hip implant itself, it is conceivable that focusing attention on the intent of an anatomical reduction—to maintain proper alignment and union among fracture pieces, would be fortuitous for device design.

Introducing a compressive element into the design of a hip screw device would potentially prevent cutout, benefit healing and ensure that fragments maintain contact through the course of patient recovery, including bone resorption.

A model of hip fracture was developed to determine if the sustained compression of a device employing a NiTi core could prevent cutout. The generated model included synthetic polyurethane foam (Sawbones, Vashon, Wa) potted in steel cylinders and loaded at an anatomic angle. The goal was to generate cutout in the model and subsequently vary insertion characteristics known to affect cutout, such as proper reduction. A prototype device incorporating a NiTi element would then be used to apply compression across the fracture site to determine if sustained compression would be effective in overcoming slightly non-anatomical reductions and preventing cutout of the screw.

The model, under conditions of poor reduction and no application of initial compression, was unable to generate cutout. Since cutout has been consistently generated clinically under the same conditions, it follows that the model used wasn't an adequate representation of the anatomical phenomenon. There are many variables in the study that could have been altered to improve the outcome. The testing material had a solid fiberglass outer layer to represent the cortical layer. While the cortex of the bone is stiffer than the trabecular bone, the stiffness of the cortex in the model masked any effects of the interaction of the softer trabecular bone between bone fragments. Effectively, any load transferred between the fragments in the fracture model was done through this fiberglass layer. A different test material with cortical layer characteristics more similar to osteoporotic cortical layer may have yielded the desired effect of cutout.

Additionally, the construct was not tested in a hydraulic testing machine, which limited the cycle speed and number.

Ultimately, the model of cutout in the hip fracture area was deemed to have too many variables to effectively demonstrate the slight difference that sustained compression via NiTi would provide. A simpler model of ankle arthrodesis was elected for to demonstrate the benefits of the incorporation of NiTi into traditional orthopaedic devices. Further work in model development would need to be done before the hip application could be effectively tested in a laboratory setting.

REFERENCES

[1] C. L. Saltzman*, et al.*, "Prospective controlled trial of STAR total ankle replacement versus ankle fusion: initial results," *Foot Ankle Int,* vol. 30, pp. 579-96, Jul 2009.

[2] L. B. Chou*, et al.*, "Tibiotalocalcaneal arthrodesis," *Foot Ankle Int,* vol. 21, pp. 804-8, Oct 2000.

[3] K. Pelton*, et al.*, "Tibiotalocalcaneal arthrodesis using a dynamically locked retrograde intramedullary nail," *Foot Ankle Int,* vol. 27, pp. 759-63, Oct 2006.

[4] M. S. Pinzur and A. Kelikian, "Charcot ankle fusion with a retrograde locked intramedullary nail," *Foot Ankle Int,* vol. 18, pp. 699-704, Nov 1997.

[5] J. A. Buckwalter*, et al.*, "The impact of osteoarthritis: implications for research," *Clin Orthop Relat Res,* pp. S6-15, Oct 2004.

[6] C. L. Saltzman*, et al.*, "Epidemiology of ankle arthritis: report of a consecutive series of 639 patients from a tertiary orthopaedic center," *Iowa Orthop J,* vol. 25, pp. 44-6, 2005.

[7] M. E. Berend*, et al.*, "A biomechanical comparison of intramedullary nail and crossed lag screw fixation for tibiotalocalcaneal arthrodesis," *Foot Ankle Int,* vol. 18, pp. 639-43, Oct 1997.

[8] J. A. Papa and M. S. Myerson, "Pantalar and tibiotalocalcaneal arthrodesis for post-traumatic osteoarthrosis of the ankle and hindfoot," *J Bone Joint Surg Am,* vol. 74, pp. 1042-9, Aug 1992.

[9] L. Dalla Paola*, et al.*, "Use of a retrograde nail for ankle arthrodesis in Charcot neuroarthropathy: a limb salvage procedure," *Foot Ankle Int,* vol. 28, pp. 967-70, Sep 2007.

[10] K. H. Salem*, et al.*, "Ankle arthrodesis using Ilizarov ring fixators: a review of 22 cases," *Foot Ankle Int,* vol. 27, pp. 764-70, Oct 2006.

[11] D. B. Thordarson*, et al.*, "Stability of an ankle arthrodesis fixed by cancellous-bone screws compared with that fixed by an external fixator. A biomechanical study," *J Bone Joint Surg Am,* vol. 74, pp. 1050-5, Aug 1992.

[12] K. Moore, D.A., *Clinically Oriented Anatomy, Fifth Edition* vol. 1208: Lippencott Williams and Wilkins, 2005.

[13] S. D. Boden*, et al.*, "An experimental lumbar intertransverse process spinal fusion model. Radiographic, histologic, and biomechanical healing characteristics," *Spine (Phila Pa 1976),* vol. 20, pp. 412-20, Feb 15 1995.

[14] H. Burchardt and W. F. Enneking, "Transplantation of bone," *Surg Clin North Am,* vol. 58, pp. 403-27, Apr 1978.

[15] D. W. Sommerfeldt and C. T. Rubin, "Biology of bone and how it orchestrates the form and function of the skeleton," *Eur Spine J,* vol. 10 Suppl 2, pp. S86-95, Oct 2001.

[16] M. Jagodzinski and C. Krettek, "Effect of mechanical stability on fracture healing--an update," *Injury,* vol. 38 Suppl 1, pp. S3-10, Mar 2007.

[17] L. E. Claes and C. A. Heigele, "Magnitudes of local stress and strain along bony surfaces predict the course and type of fracture healing," *J Biomech,* vol. 32, pp. 255-66, Mar 1999.

[18] J. Kenwright and A. E. Goodship, "Controlled mechanical stimulation in the treatment of tibial fractures," *Clin Orthop Relat Res,* pp. 36-47, Apr 1989.

[19] J. Charnley, "Compression arthrodesis of the ankle and shoulder," *J Bone Joint Surg Br,* vol. 33B, pp. 180-91, May 1951.

[20] Fink, "Reasons for non-unions after arthrodeses of the ankle," *Foot and Ankle Surgery,* vol. 2, pp. 145-154, 1996.

[21] T. M. Mueckley*, et al.*, "Biomechanical evaluation of primary stiffness of tibiotalar arthrodesis with an intramedullary compression nail and four other fixation devices," *Foot Ankle Int,* vol. 27, pp. 814-20, Oct 2006.

[22] J. C. Adams, "Arthrodesis of the ankle joint; experiences with the transfibular approach," *J Bone Joint Surg Br,* vol. 30B, pp. 506-11, Aug 1948.

[23] C. M. Yakacki*, et al.*, "Compression forces of internal and external ankle fixation devices with simulated bone resorption," *Foot Ankle Int,* vol. 31, pp. 76-85, Jan 2010.
[24] F. J. Gil and J. A. Planell, "Shape memory alloys for medical applications," *Proc Inst Mech Eng H,* vol. 212, pp. 473-88, 1998.
[25] J. Richmond*, et al.*, "Mortality risk after hip fracture. 2003," *J Orthop Trauma,* vol. 17, pp. S2-5, Sep 2003.
[26] B. Gullberg*, et al.*, "World-wide projections for hip fracture," *Osteoporos Int,* vol. 7, pp. 407-13, 1997.
[27] A. H. Schmidt and M. F. Swiontkowski, "Femoral neck fractures," *Orthop Clin North Am,* vol. 33, pp. 97-111, viii, Jan 2002.
[28] J. J. Roche*, et al.*, "Effect of comorbidities and postoperative complications on mortality after hip fracture in elderly people: prospective observational cohort study," *BMJ,* vol. 331, p. 1374, Dec 10 2005.
[29] O. Johnell and J. A. Kanis, "An estimate of the worldwide prevalence, mortality and disability associated with hip fracture," *Osteoporos Int,* vol. 15, pp. 897-902, Nov 2004.
[30] M. J. Parker, "Inter-hospital variations in length of hospital stay following hip fracture," *Age and Ageing,* vol. 27, pp. 333-337, 1998.
[31] G. S. Keene*, et al.*, "Mortality and morbidity after hip fractures," *BMJ,* vol. 307, pp. 1248-50, Nov 13 1993.
[32] R. S. Braithwaite*, et al.*, "Estimating hip fracture morbidity, mortality and costs," *J Am Geriatr Soc,* vol. 51, pp. 364-70, Mar 2003.
[33] N. F. Ray*, et al.*, "Medical expenditures for the treatment of osteoporotic fractures in the United States in 1995: report from the National Osteoporosis Foundation," *J Bone Miner Res,* vol. 12, pp. 24-35, Jan 1997.
[34] C. J. Hsu*, et al.*, "Hemi-arthroplasty with supplemental fixation of greater trochanter to treat failed hip screws of femoral intertrochanteric fracture," *Arch Orthop Trauma Surg,* vol. 128, pp. 841-5, Aug 2008.
[35] G. D. Krischak*, et al.*, "Biomechanical comparison of two side plate fixation techniques in an unstable intertrochanteric osteotomy model: Sliding Hip Screw and Percutaneous Compression Plate," *Clin Biomech (Bristol, Avon),* vol. 22, pp. 1112-8, Dec 2007.
[36] W. Schumpelick and P. M. Jantzen, "A new principle in the operative treatment of trochanteric fractures of the femur," *J Bone Joint Surg Am,* vol. 37-A, pp. 693-8, Jul 1955.
[37] A. H. Simpson*, et al.*, "Sliding hip screws: modes of failure," *Injury,* vol. 20, pp. 227-31, Jul 1989.
[38] S. C. Halder, "The Gamma nail for peritrochanteric fractures," *J Bone Joint Surg Br,* vol. 74, pp. 340-4, May 1992.
[39] K. S. Leung*, et al.*, "Gamma nails and dynamic hip screws for peritrochanteric fractures. A randomised prospective study in elderly patients," *J Bone Joint Surg Br,* vol. 74, pp. 345-51, May 1992.
[40] L. Ahrengart*, et al.*, "A randomized study of the compression hip screw and Gamma nail in 426 fractures," *Clin Orthop Relat Res,* pp. 209-22, Aug 2002.
[41] M. J. Parker and H. H. Handoll, "Gamma and other cephalocondylic intramedullary nails versus extramedullary implants for extracapsular hip fractures in adults," *Cochrane Database Syst Rev,* p. CD000093, 2008.
[42] J. O. Anglen and J. N. Weinstein, "Nail or plate fixation of intertrochanteric hip fractures: changing pattern of practice. A review of the American Board of Orthopaedic Surgery Database," *J Bone Joint Surg Am,* vol. 90, pp. 700-7, Apr 2008.

[43] S. H. Bridle*, et al.*, "Fixation of intertrochanteric fractures of the femur. A randomised prospective comparison of the gamma nail and the dynamic hip screw," *J Bone Joint Surg Br,* vol. 73, pp. 330-4, Mar 1991.
[44] P. J. Radford*, et al.*, "A prospective randomised comparison of the dynamic hip screw and the gamma locking nail," *J Bone Joint Surg Br,* vol. 75, pp. 789-93, Sep 1993.
[45] I. B. Schipper*, et al.*, "Treatment of unstable trochanteric fractures. Randomised comparison of the gamma nail and the proximal femoral nail," *J Bone Joint Surg Br,* vol. 86, pp. 86-94, Jan 2004.
[46] R. Stern, "Are there advances in the treatment of extracapsular hip fractures in the elderly?," *Injury,* vol. 38 Suppl 3, pp. S77-87, Sep 2007.
[47] A. Moroni*, et al.*, "HA-coated screws decrease the incidence of fixation failure in osteoporotic trochanteric fractures," *Clin Orthop Relat Res,* pp. 87-92, Aug 2004.
[48] C. H. Crawford*, et al.*, "The trochanteric nail versus the sliding hip screw for intertrochanteric hip fractures: a review of 93 cases," *J Trauma,* vol. 60, pp. 325-8; discussion 328-9, Feb 2006.
[49] M. R. Baumgaertner*, et al.*, "The value of the tip-apex distance in predicting failure of fixation of peritrochanteric fractures of the hip," *J Bone Joint Surg Am,* vol. 77, pp. 1058-64, Jul 1995.
[50] A. L. Utrilla*, et al.*, "Trochanteric gamma nail and compression hip screw for trochanteric fractures: a randomized, prospective, comparative study in 210 elderly patients with a new design of the gamma nail," *J Orthop Trauma,* vol. 19, pp. 229-33, Apr 2005.
[51] J. A. Geller*, et al.*, "Tip-apex distance of intramedullary devices as a predictor of cut-out failure in the treatment of peritrochanteric elderly hip fractures," *Int Orthop,* vol. 34, pp. 719-22, Jun 2010.